

Automated Security Response through Online Learning with Adaptive Conjectures

Kim Hammar[†], Tao Li[‡], Rolf Stadler[†], and Quanyan Zhu[‡]

[†] Division of Network and Systems Engineering, KTH Royal Institute of Technology, Sweden

[‡] Department of Electrical and Computer Engineering, New York University, USA

Email: {kimham, stadler}@kth.se, {tl2636, qz494}@nyu.edu

January 7, 2025

Abstract—We study automated security response for an IT infrastructure and formulate the interaction between an attacker and a defender as a partially observed, non-stationary game. We relax the standard assumption that the game model is correctly specified and consider that each player has a probabilistic conjecture about the model, which may be misspecified in the sense that the true model has probability 0. This formulation allows us to capture uncertainty and misconception about the infrastructure and the intents of the players. To learn effective game strategies online, we design Conjectural Online Learning (COL), a novel method where a player iteratively adapts its conjecture using Bayesian learning and updates its strategy through rollout. We prove that the conjectures converge to best fits, and we provide a bound on the performance improvement that rollout enables with a conjectured model. To characterize the steady state of the game, we propose a variant of the Berk-Nash equilibrium. We present COL through an advanced persistent threat use case. Testbed evaluations show that COL produces effective security strategies that adapt to a changing environment. We also find that COL enables faster convergence than current reinforcement learning techniques.

Index Terms—Cybersecurity, network security, APT, game theory, Berk-Nash equilibrium, Bayesian learning, rollout.

I. INTRODUCTION

AN organization’s security strategy has traditionally been defined and updated by domain experts. Though this approach can provide basic security for an organization’s IT infrastructure, a growing concern is that infrastructure update cycles become shorter and attacks increase in sophistication. To address this challenge, game-theoretic methods for automating security strategies have been proposed, whereby the interaction between an attacker and a defender is modeled as a game [1]; see Fig. 1. While such methods can produce optimal security strategies, they rely on unrealistic assumptions about the infrastructure. In particular, most of the current methods are limited to stationary and correctly specified games, which assume a static infrastructure that can be accurately modeled without misspecification [2]–[11]. These assumptions are unrealistic for several reasons.

First, IT infrastructures are *dynamic*: components fail, software packages are updated, new vulnerabilities are discovered, etc. As a consequence, the game between the attacker and the defender is *non-stationary*. Second, attackers and defenders often have incorrect prior knowledge about the infrastructure and the opponent, which means that players generally have

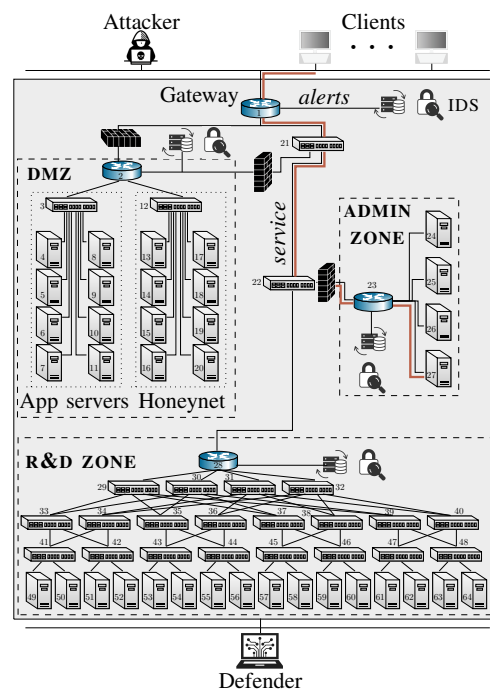


Fig. 1: The target infrastructure and the actors involved in the Advanced Persistent Threat (APT) use case.

misspecified models. Third, the defender has limited knowledge about an attacker’s presence and actions, which means that the game has *partial observability*.

Motivating example: the NOTPETYA attack. NOTPETYA is a malware that was used by the SANDWORM Advanced Persistent Threat (APT) in a worldwide attack in 2017 [12]. Security researchers initially conjectured that NOTPETYA was a version of the PETYA ransomware (hence the name) [13]. As a result, many organizations focused on traditional ransomware response strategies. However, it later became evident that the malware was not financially motivated but designed for destruction. This misspecification delayed effective responses.

In this paper, we address the above challenges and present Conjectural Online Learning (COL), a game-theoretic method for *online learning* of security strategies that applies to dynamic IT environments where attackers and defenders have misconceptions about the environment and the opponent’s

strategy. Using this method, we formulate the interaction between an attacker and a defender as a non-stationary, partially observed game. We relax the standard assumption that the game model is correctly specified and consider the case where each player has a probabilistic *conjecture* about the model, i.e., a probability distribution over possible models, which may be *misspecified* in the sense that the true model has probability 0. Both players iteratively adapt their conjecture using *Bayesian learning* and update their strategies using *rollout*, which is a form of approximate dynamic programming [14]; see Fig. 2. We prove that the conjectures converge to best fits, and we provide a bound on the performance improvement that rollout enables with a conjectured model. To characterize the steady state of the game, we define a variant of the *Berk-Nash equilibrium* [15, Def. 1], which represents a fixed point where players act optimally given their conjectures.

While the study of learning with misspecified models has attracted long-standing interest in economics [15], engineering [16], and psychology [17], it remains unexplored in the security context. Related research in the security literature include (i) game-theoretic approaches based on bounded rationality [11], [18]–[28]; (ii) game-theoretic approaches based on imperfect and incomplete information [8], [29]–[32]; and (iii) model-free learning techniques [4], [8], [9], [30], [33]–[39]. (A review of related work can be found in §VIII.) To our knowledge, we provide the first study of learning with misspecified models in a security context. The benefit of this approach is threefold. First, it provides a new methodology to capture uncertainty and misspecification in security games. Second, as we show in this paper, it applies to dynamic, non-stationary, and partially observed games. Third, the model conjectures produced by our method are guaranteed to converge under reasonable conditions, and the worst-case performance of the learned strategies is bounded.

We present our method (COL) through a use case that involves an APT on an IT infrastructure; see Fig. 1. We emulate this infrastructure with a *digital twin*, on which we run APT actions and defender responses. (A video demonstration of the digital twin is available at [40].) During such runs, we collect measurements and logs, from which we estimate infrastructure statistics. This data is then used to instantiate simulations of the use case, based on which we evaluate the performance of COL. We find that COL produces effective security strategies that adapt to a changing environment. The simulations also show that COL enables faster convergence than current reinforcement learning techniques. In addition to the simulation studies, we evaluate COL on the digital twin and compare it against the SNORT Intrusion Detection and Prevention System (IDPS) [41]. The results attest that COL adapts to changes in the distribution of network traffic and outperforms SNORT in several key metrics, e.g., percentage of blocked attack attempts and throughput of client requests.

Contributions.

- 1) We introduce a novel game-theoretic formulation for the problem of automated security response where each player (i.e., attacker or defender) has a probabilistic conjecture about the game model. This formulation allows

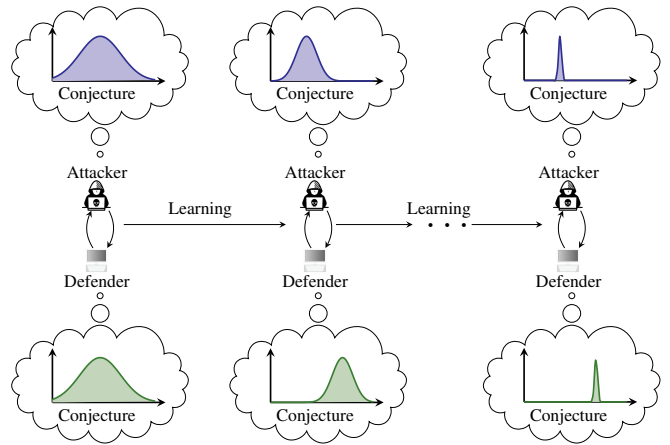


Fig. 2: **Conjectural Online Learning (COL)**: each player adapts a (possibly misspecified) conjecture about the game model through Bayesian learning.

us to capture model misspecification and uncertainty.

- 2) We present COL, a new method for online learning of game strategies where a player iteratively adapts its conjecture using Bayesian learning and updates its strategy through rollout. This method allows us to automatically adapt security strategies to changes in the environment.
- 3) We prove that, when using COL, the conjectures of both players converge, and we characterize the steady state as a variant of the *Berk-Nash equilibrium* [15, Def. 1]. We also provide a bound on the performance improvement that rollout enables with a conjectured model.
- 4) We evaluate COL using simulation and emulation studies based on a digital twin running 64 virtualized servers and 10 different types of APTs [40]. This evaluation provides insights into how COL performs under different conditions and shows that it converges faster than current reinforcement learning techniques. It also shows that COL outperforms the SNORT IDPS in several key metrics [41].

Software and data availability. Source code of our platform for creating digital twins and a dataset of 6400 APT traces are available in the repository at [40]. This repository also includes container images that implement the APTs and the response actions used in our experimental evaluation.

II. USE CASE: ADVANCED PERSISTENT THREAT (APT)

We consider the problem of defending an organization’s IT infrastructure against an APT caused by an *attacker* [42]. The operator of the infrastructure, which we call the *defender*, takes measures to protect it against the attacker while providing services to a client population; see Fig. 1. The infrastructure includes a set of servers and an Intrusion Detection System (IDS) that logs events in real-time. Clients access the services through a public gateway, which is also open to the attacker.

The attacker aims to intrude on the infrastructure over an extended period. It begins with reconnaissance to identify vulnerabilities, after which it attempts to compromise servers through exploits. Once inside the infrastructure, the attacker employs lateral movement techniques, escalates privileges, and uses advanced evasion tactics to avoid detection.

The defender monitors the infrastructure by observing IDS alerts and other statistics. It can recover potentially compromised servers (e.g., by upgrading their software), which temporarily disrupts service for clients. When deciding to take this response action, the defender balances two conflicting objectives: (i) maintain services to its clients; and (ii) recover compromised servers.

III. GAME MODEL OF THE APT USE CASE

We formulate the above use case as a zero-sum stochastic game with one-sided partial observability

$$\Gamma \triangleq \langle \mathcal{N}, \mathcal{S}, (\mathcal{A}_k)_{k \in \mathcal{N}}, f, c, \gamma, \mathbf{b}_1, \mathcal{O}, z \rangle, \quad (1)$$

where \mathcal{N} is the set of players, \mathcal{S} is the set of states, $(\mathcal{A}_k)_{k \in \mathcal{N}}$ are the sets of actions, and \mathcal{O} is the set of observations; f is the transition function, c is the cost function, and z is the observation function; γ is the discount factor; and \mathbf{b}_1 is the initial state distribution [43, Def. 3.1]. Γ is a discrete-time game with two players: the (D)efender and the (A)ttacker.

The attacker and the defender have different observability in the game. The defender observes IDS alerts but has no certainty about an attacker's presence. (While we focus on the IDS alert metric in this paper, our model can be used with alternative sources of metrics, e.g., information flow tracking [42], [44].) The attacker, on the other hand, has complete observability. It has access to all the information the defender has access to and the defender's past actions. We can motivate this assumption in several ways. First, the assumption holds for insider attacks [8]. Second, it reflects that it is generally not known what information is available to the attacker [43]. Third, it reduces the computational complexity of solving the game [45], [46].

In the following subsections, we define the components of the game, its evolution, and the players' objectives.

Notation. Boldface lower case letters (e.g., $\mathbf{x} = (x_1, x_2, \dots)$) denote column vectors. \mathbf{e}_i is the i -th standard basis vector. Upper case calligraphy letters (e.g., \mathcal{V}) represent sets. \mathbb{P} is a probability measure. (The construction of the underlying probability space is standard and shall be omitted for brevity.) The set of probability distributions over \mathcal{V} is written as $\Delta(\mathcal{V})$. $\mathbb{1}$ is the indicator function. $\delta_i(\cdot)$ is the Dirac delta function. A random variable is written in upper case (e.g., X), a random vector in boldface (e.g., \mathbf{X}). The expectation of f with respect to X is written as $\mathbb{E}_X[f]$. $x \sim f$ means that x is sampled from f . If the expression f includes many random variables that depend on π , we write $\mathbb{E}_\pi[f]$. We use $\mathbb{P}[x|y]$ as a shorthand for $\mathbb{P}[X = x|Y = y]$ and $-k$ as a shorthand for $\mathcal{N} \setminus \{k\}$. Further notation is listed in Table 1.

A. Actions

Both players can invoke two actions: (S)top and (C)ontinue. The action spaces are thus $\mathcal{A}_D \triangleq \mathcal{A}_A \triangleq \{S, C\}$. S triggers a change in the game state while C is a passive action that does not change the state. Specifically, $a_t^{(A)} = S$ is the attacker's compromise action, and $a_t^{(D)} = S$ is the defender's recovery action (as defined in the use case §II).

Notation(s)	Description
Γ, c, N	The game (1), cost function (7), and # servers (§III-B)
D, A	The defender player and the attacker player (1)
$\mathcal{N}, \mathcal{S}, \mathcal{O}$	Sets of players, states, and observations (1)
$\mathcal{A}_D, \mathcal{A}_A$	Sets of defender and attacker actions (1)
t, γ	Time step and discount factor (8)
π_D, π_A	Defender and attacker strategies (§III-D)
$\Pi = \Pi_D \times \Pi_A$	Defender and attacker strategy spaces (§III-D)
$\tilde{\pi}_D, \tilde{\pi}_A$	Best response strategies
$\boldsymbol{\pi}^* = (\pi_D^*, \pi_A^*)$	Nash equilibrium strategies (11)
$\mathcal{B}_D, \mathcal{B}_A$	Best response correspondences
J_D, J_A	Defender and attacker objectives (8)
f, z	Transition function (2) and observation function (4)
s_t, o_t	State (2) and observation (4) at time t
$\mathbf{a}_t = (a_t^{(D)}, a_t^{(A)})$	Actions at time t (§III-A)
S_t, O_t	Random variables with realizations s_t (2) and o_t (4)
\mathbf{A}_t	Random vector with realization \mathbf{a}_t (§III-A)
$\mathbf{b}_t, \mathbf{B}_t$	Defender belief (\mathbf{b}_t realizes the random vector \mathbf{B}_t) (5)
\mathcal{B}, \mathbf{B}	Belief space and belief operator of the defender (6)
$\mathbf{h}_t^{(k)}, \mathbf{h}_t$	History of player k and joint history (§III-C)
$\mathbf{H}_t^{(k)}, \mathbf{H}_t$	Random vectors with realizations $\mathbf{h}_t^{(k)}$ and \mathbf{h}_t (§III-C)
$\mathcal{H}_t = \mathcal{H}_t^{(D)} \times \mathcal{H}_t^{(A)}$	History spaces (§III-C)
\mathcal{S}, \mathcal{C}	Stop and continue actions (§III-A)
\mathcal{R}	Rollout operator for online learning (13)
$\tilde{\pi}_{-k,t}$	Player k 's conjecture of player $-k$'s strategy (Alg. 1)
ℓ_D, ℓ_A	Lookahead horizons (Alg. 1)
$\bar{\ell}_{-k,t}$	Player k 's conjecture of player $-k$'s lookahead (Alg. 1)
$\boldsymbol{\theta}_t$	Parameter vector of Γ at time t (15a)
$\bar{\boldsymbol{\theta}}_t^{(k)}$	Player k 's conjecture of $\boldsymbol{\theta}_t$ at time t (15a)
\mathcal{L}, Θ_k	Player k 's sets of possible conjectures of ℓ_A and $\boldsymbol{\theta}$ (15)
$\mathcal{L}^*, \Theta_k^*$	Sets of consistent conjectures (17)
$\mathbf{i}_t^{(k)}, \mathbf{i}_t^{(k)}$	Information feedback of player k at time t (3)
$\mu_t, \rho_t^{(k)}$	Posteriors $\mathbb{P}[\ell_A \mathbf{h}_t^{(D)}]$ (15b) and $\mathbb{P}[\boldsymbol{\theta}_t^{(k)} \mathbf{h}_t^{(A)}]$ (15a)
$\nu, K(\bar{\alpha}, \nu)$	Occupancy measure and discrepancy of conjecture $\bar{\alpha}$ (16)
$\pi_{1,k}, \pi_{t,k}$	Base and rollout strategy of player k at time t (13)
$\boldsymbol{\pi}_{\mathbf{h}_t}$	Strategy profile induced by Alg. 1 at time t (§V-A)
$\mathbb{P}^{\mathcal{R}}$	Distribution over $\prod_{t \geq 1} (\mathcal{H}_t^{(D)} \times \mathcal{H}_t^{(A)})$ (Thm. 4)
$K_{\mathcal{L}}^*, K_{\Theta_k}^*$	Minimal discrepancy values for \mathcal{L} and Θ_k (17)

TABLE 1: Notation.

B. Dynamics

The state $s_t \in \mathcal{S} \triangleq \{0, 1, \dots, N\}$ represents the number of compromised servers at time t , where $s_1 = 0$. The transition $s_t \rightarrow s_{t+1}$ occurs with probability $f(s_{t+1} | s_t, a_t^{(D)}, a_t^{(A)})$:

$$f(s_{t+1} = 0 | s_t, S, a_t^{(A)}) \triangleq 1 \quad (2a)$$

$$f(s_{t+1} = s_t | s_t, C, C) \triangleq f(s_{t+1} = N | N, C, S) \triangleq 1 \quad (2b)$$

$$f(s_{t+1} = s_t | s_t, C, S) \triangleq 1 - p_A \quad s_t < N \quad (2c)$$

$$f(s_{t+1} = s_t + 1 | s_t, C, S) \triangleq p_A \quad s_t < N, \quad (2d)$$

where p_A is the probability of a successful attack. All other transitions have probability 0; see Fig. 3.

(2a) defines the transition $s_t \rightarrow 0$, which occurs when the defender takes action S. (2b)–(2c) define the recurrent transition $s_{t+1} = s_t$, which occurs when both players take action C or when the attacker is unsuccessful in compromising a server, which happens with probability $1 - p_A$. Lastly, (2d) defines the transition $s_t \rightarrow s_t + 1$, which occurs with probability p_A when the attacker takes action S and the defender takes action C.

C. Observability

The attacker has complete observability. It knows the game state, the defender's actions, and the defender's observations. In contrast, the defender has a finite set of observations $o_t \in$

$$\mathbb{B}(\mathbf{b}_{t-1}, a_{t-1}^{(D)}, o_t, \pi_A)(s_t) \triangleq \frac{z(o_t | s_t) \sum_{s_{t-1} \in \mathcal{S}} \sum_{a_{t-1}^{(A)} \in \mathcal{A}_A} \pi_A(a_{t-1}^{(A)} | \mathbf{b}_{t-1}, s_{t-1}) \mathbf{b}_{t-1}(s_{t-1}) f(s_t | s_{t-1}, a_{t-1}^{(D)}, a_{t-1}^{(A)})}{\sum_{a_{t-1}^{(A)} \in \mathcal{A}_A} \sum_{s', s \in \mathcal{S}} z(o_t | s') \pi_A(a_{t-1}^{(A)} | s, \mathbf{b}_{t-1}) f(s' | s, a_{t-1}^{(D)}, a_{t-1}^{(A)}) \mathbf{b}_{t-1}(s)}. \quad (6)$$

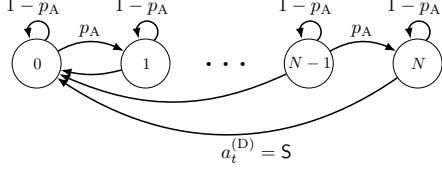


Fig. 3: State transition diagram of the game: disks represent states; arrows represent state transitions; labels indicate probabilities and conditions for state transition; the initial state is $s_1 = 0$.

\mathcal{O} . Consequently, the *information feedbacks* for the attacker and the defender at time t are

$$\mathbf{i}_t^{(A)} \triangleq (o_t, s_t, a_{t-1}^{(D)}) \quad \text{and} \quad \mathbf{i}_t^{(D)} \triangleq (o_t), \quad (3)$$

respectively, where o_t is drawn from a random variable O_t whose distribution depends on the clients and the state, i.e.,

$$o_t \sim z(\cdot | s_t). \quad (4)$$

Each player k has *perfect recall* [47, Def. 7], which means that it remember the play history $\mathbf{h}_t^{(k)} \triangleq (\mathbf{b}_1, a_l^{(k)}, \mathbf{i}_l^{(k)})_{l=1,2,\dots} \in \mathcal{H}_t^{(k)}$. Based on this history, the defender computes the *belief state* $\mathbf{b}_t \in \mathcal{B}$, which is defined as

$$\mathbf{b}_t(s_t) \triangleq \mathbb{P}[S_t = s_t | \mathbf{h}_t^{(D)}], \quad (5)$$

where \mathbf{b}_t is computed recursively through the operator \mathbb{B} (6), which is defined at the top of the page.

D. Strategies and Objectives

Since \mathbf{b}_t is a sufficient statistic for the Markovian state s_t (2) [48, Def. 4.2, Lem. 5.1, Thm. 7.1], we can define the players' *behavior Markov strategies* as $\pi_D \in \Pi_D \triangleq \mathcal{B} \rightarrow \Delta(\mathcal{A}_D)$ and $\pi_A \in \Pi_A \triangleq \mathcal{B} \times \mathcal{S} \rightarrow \Delta(\mathcal{A}_A)$ [47, Def. 5]. Their performances are quantified using the cost function

$$c(s_t, a_t^{(D)}) \triangleq \overbrace{s_t^p \mathbb{1}_{a_t^{(D)} \neq S}}^{\text{intrusion cost}} + \overbrace{\mathbb{1}_{a_t^{(D)} = S} (q - r \mathbb{1}_{s_t > 0})}^{\text{response action cost}}, \quad (7)$$

where $p \geq 1$, $q > 0$, and $r > 0$ are scalar constants satisfying $1 > q - r$; see Fig. 4. The first term in (7) encodes the intrusion cost s_t^p , which increases with the number of compromised servers s_t . The second term encodes the stop action cost, which is $q - r$ if an intrusion occurs and q otherwise.

The goal of the defender is to *minimize* the expected cumulative cost, and the goal of the attacker is to *maximize* the same quantity. Therefore, the objective functions are

$$J_D^{(\pi_D, \pi_A)}(\mathbf{b}_1) \triangleq \mathbb{E}_{(\pi_D, \pi_A)} \left[\sum_{t=1}^{\infty} \gamma^{t-1} c(S_t, A_t^{(D)}) | \mathbf{b}_1 \right] \quad (8a)$$

$$J_A^{(\pi_D, \pi_A)}(\mathbf{b}_1) \triangleq -J_D^{(\pi_D, \pi_A)}(\mathbf{b}_1), \quad (8b)$$

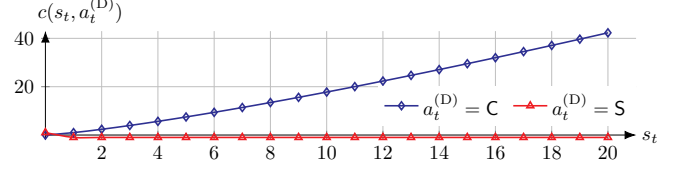


Fig. 4: An example cost function $c(s_t, a_t^{(D)})$ (7) of Γ (1); hyperparameters are listed in Appendix F

where $\gamma \in [0, 1)$ is a discount factor and $\mathbb{E}_{(\pi_D, \pi_A)}$ is the expectation over the random vectors $(\mathbf{H}_t^{(D)}, \mathbf{H}_t^{(A)})_{t \in \{1, 2, \dots\}}$ when the game is played according to (π_D, π_A) .

A defender strategy $\tilde{\pi}_D \in \Pi_D$ is a *best response* against $\pi_A \in \Pi_A$ if it *minimizes* $J_D^{(\pi_D, \pi_A)}$ (8a). Similarly, an attacker strategy $\tilde{\pi}_A$ is a best response against π_D if it *maximizes* $J_D^{(\pi_D, \pi_A)}$ (8b). Hence, the best response correspondences are

$$\mathcal{B}_D(\pi_A) \triangleq \arg \min_{\pi_D \in \Pi_D} J_D^{(\pi_D, \pi_A)}(\mathbf{b}_1) \quad (9a)$$

$$\mathcal{B}_A(\pi_D) \triangleq \arg \max_{\pi_A \in \Pi_A} J_D^{(\pi_D, \pi_A)}(\mathbf{b}_1). \quad (9b)$$

When the infrastructure contains a single server ($N = 1$), there exist *best responses* with *threshold structure*, as stated below.

Theorem 1. *If $N = 1$, then*

(A) *For any $\pi_A \in \Pi_A$, there exists a value $\alpha^* \in [0, 1]$ and a best response $\tilde{\pi}_D \in \mathcal{B}_D(\pi_A)$ (9a) that satisfies*

$$\tilde{\pi}_D(\mathbf{b}) = S \iff \mathbf{b}(1) \geq \alpha^*. \quad (10a)$$

(B) *Assuming $\pi_A(0, \mathbf{e}_1) = S \forall \pi_A \in \Pi_A$. Then, for any $\pi_D \in \Pi_D$ that satisfies (10a), there exists a value $\beta^* \in [0, 1]$ and a best response $\tilde{\pi}_A \in \mathcal{B}_A(\pi_D)$ (9b) that satisfies*

$$\tilde{\pi}_A(s, \mathbf{b}) = S \iff s = 0, \mathbf{b}(1) \leq \beta^*. \quad (10b)$$

The above theorem implies that when $N = 1$, the *best responses* can be parameterized by thresholds, which allows formulating (9a)–(9b) as parametric optimization problems. Figure 5 shows the convergence curves when performing these optimizations with the **Cross-Entropy Method** (CEM) [50]. We provide the proof in Appendix A.

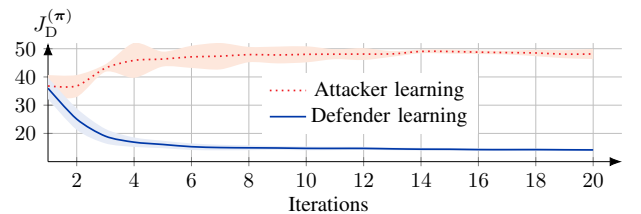


Fig. 5: *Best response* learning when $N = 1$ using CEM [50] and the threshold parameterization expressed in Thm. 1; the curves show the mean and the 95% confidence interval from evaluations with 20 random seeds; hyperparameters are listed in Appendix F.

E. Equilibria

When the attacker and the defender play **best responses**, their strategy pair is a *Nash equilibrium* [51, Eq. 1] and can be written as

$$\pi^* \triangleq (\pi_D^*, \pi_A^*) \in \mathcal{B}_D(\pi_A^*) \times \mathcal{B}_A(\pi_D^*). \quad (11)$$

This equilibrium solves the following minimax problem [52].

$$\underset{\pi_D \in \Pi_D}{\text{minimize}} \underset{\pi_A \in \Pi_A}{\text{maximize}} J_D^{(\pi_D, \pi_A)}(\mathbf{b}_1) \quad (12a)$$

$$\text{subject to } s_{t+1} \sim f(\cdot | s_t, \mathbf{a}_t) \quad \forall t \quad (12b)$$

$$o_t \sim z(\cdot | s_t) \quad \forall t \quad (12c)$$

$$a_t^{(A)} \sim \pi_A(\cdot | s_t, \mathbf{b}_t) \quad \forall t \quad (12d)$$

$$a_t^{(D)} \sim \pi_D(\cdot | \mathbf{b}_t) \quad \forall t \quad (12e)$$

$$s_1 \sim \mathbf{b}_1, \quad (12f)$$

where (12b) is the dynamics constraint; (12c) describes the observations; (12d)–(12e) capture the actions; and (12f) defines the initial state distribution. (Remark: As a solution to (12) exists [46, Thm. 2.3], we write min max instead of inf sup.)

While any strategy pair π^* that satisfies (11) is a Nash equilibrium, (12) implies that π^* together with \mathbb{B} (6) can form a stronger equilibrium, namely a *perfect Bayesian equilibrium*.

Definition 1 (Perfect Bayesian equilibrium [53], [54]). π^* (11) and \mathbb{B} (6) is a *perfect Bayesian equilibrium* iff

1) π^* is a Nash equilibrium in $\Gamma|_{\mathbf{h}_t^{(D)}} \forall \mathbf{h}_t^{(D)} \in \mathcal{H}_t^{(D)}$,

where $\Gamma|_{\mathbf{h}_t^{(D)}}$ is the subgame starting from $\mathbb{B}(\mathbf{h}_t^{(D)}, \pi_A^*)$.

2) For any $\mathbf{h}_t^{(D)} \in \mathcal{H}_t^{(D)}$ with $\mathbb{P}[\mathbf{h}_t^{(D)} | \pi^*, \mathbf{b}_1] > 0$, then

$$\mathbb{B}(\mathbf{h}_t^{(D)}, \pi_A^*) = \mathbb{B}(\mathbb{B}(\mathbf{h}_{t-1}^{(D)}, \pi_A^*), \pi_D^*(\mathbb{B}(\mathbf{h}_{t-1}^{(D)}, \pi_A^*), o_t, \pi_A^*)).$$

Theorem 2. Given the instantiation of Γ described in §III, the following holds.

(A) $|\mathcal{B}_D(\pi_A)| > 0$ and $|\mathcal{B}_A(\pi_D)| > 0 \forall (\pi_A, \pi_D)$.

(B) Γ has a *perfect Bayesian equilibrium*.

Proof. Since Γ is finite and $\gamma \in [0, 1)$, (A) follows from [49, Thms. 7.6.1–7.6.2][55, Thm. 6, p. 160]. We omit the proof as it is standard in Markov decision theory. Readers familiar with the literature are encouraged to consult [49] for the details. We prove (B) by construction. For any *reachable* subgame, a Nash equilibrium π^* exists [56, §3][46, Thm. 2.3]. For any *unreachable* subgame $\Gamma|_{\mathbf{h}_j^{(D)}}$, we can construct another Nash equilibrium $\pi^{*,j}$. This follows because the proofs in [56, §3][46, Thm. 2.3] do not depend on \mathbf{b}_1 . By combining π^* with the equilibria of all unreachable subgames, we obtain a *perfect Bayesian equilibrium*. \square

Figure 6 shows the value of a *perfect Bayesian equilibrium* when $N = 1$. Interestingly, the defender has the highest expected cost when the belief of compromise ($\mathbf{b}(1)$) is around 0.35 rather than 0.5.

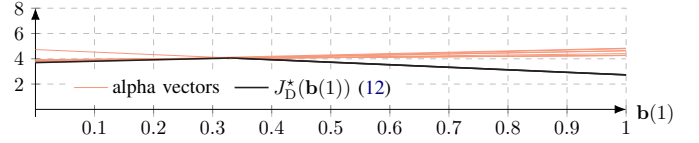


Fig. 6: The equilibrium value (12) of Γ when $N = 1$ (computed with the HSVI algorithm [57, Alg. 1]); $J_D^*(\mathbf{b}(1)) = \min_i [1 - \mathbf{b}(1), \mathbf{b}(1)]^T \boldsymbol{\alpha}^{(i)}$, where $\boldsymbol{\alpha}^{(i)}$ is an *alpha vector* [58, Def. 1]; see Appendix F for the hyperparameters.

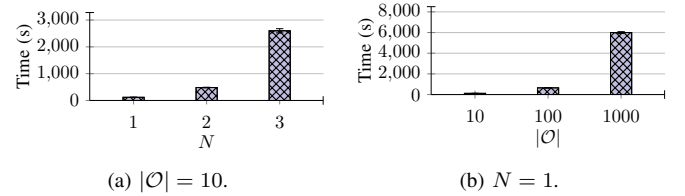


Fig. 7: Time required to compute a *perfect Bayesian equilibrium* of Γ (1) with HSVI [57, Alg. 1] for different values of N (Fig. 7a) and $|\mathcal{O}|$ (Fig. 7b); error bars indicate the 95% confidence interval based on 20 measurements; hyperparameters are listed in Appendix F.

IV. PROBLEM STATEMENT

While the equilibrium defined above describes how the game *ought to be played* by rational players, computing it is generally intractable, as illustrated in Fig. 7. Further, the equilibrium assumes a stationary game where players have correctly specified models, which is not the case in practice. To address these limitations, we relax the standard assumptions and consider a setting where the game is *non-stationary* and players have *misspecified* models, as described below.

Problem 1 (Non-stationary game with misspecification). We consider a game $\Gamma_{\boldsymbol{\theta}_t}$ based on (1) that is parameterized by a time-dependent vector $\boldsymbol{\theta}_t$, which is hidden from the players. This vector can represent the transition function (2), the observation function (4), etc. (The game parameters of (1) that are not included in $\boldsymbol{\theta}_t$ are defined in §III and known to both players.) Player k has a *conjecture* of $\boldsymbol{\theta}_t$, denoted by $\bar{\boldsymbol{\theta}}_t^{(k)} \in \Theta_k$, which is *misspecified* if $\boldsymbol{\theta}_t \notin \Theta_k$. As $\boldsymbol{\theta}_t$ evolves, player k adapts its conjecture based on feedback $\mathbf{i}_t^{(k)}$ (3) and uses the conjecture to update its strategy $\pi_{k,t}$, starting from a *base strategy* $\pi_{k,1}$. (Note that we do not make any assumption about the time evolution of $\boldsymbol{\theta}_t$.) Strategy updates are parameterized by a *lookahead horizon* ℓ_k , which can be understood as a computational constraint. The defender conjectures ℓ_A as $\bar{\ell}_A \in \mathcal{L}$, which captures the defender’s uncertainty about the attacker’s computational capacity. We assume the attacker knows ℓ_D and the defender’s conjectures.

We illustrate Prob. 1 using the following example.

Example: Moving target defense.

The attacker has performed reconnaissance and knows the game model (1), i.e., $\Theta_A = \{\boldsymbol{\theta}_1\}$. However, the configuration changes regularly $\boldsymbol{\theta}_1 \rightarrow \boldsymbol{\theta}_2 \rightarrow \dots$ via a moving target defense scheme, leading to a misspecified model.

Solving [Prob. 1](#) leads to the following questions.

- ❓ What is an effective method for a player to update its conjecture and its strategy?
- ❓ Do the sequences of conjectures converge?
- ❓ Once the parameters θ_t remain constant, how can the steady state of Γ_{θ_t} be characterized?

V. ONLINE LEARNING WITH ADAPTIVE CONJECTURES

We address the above questions and develop **Conjectural Online Learning (COL)**, a game-theoretic method for *online learning* in Γ_{θ_t} ([Prob. 1](#)). Using **COL**, each player iteratively adapts its conjecture through *Bayesian learning* and updates its strategy through *rollout*, which is a form of approximate dynamic programming; see [Fig. 8](#) [[14](#)]. The pseudocode of **COL** is listed in [Alg. 1](#) and the main steps are described below.

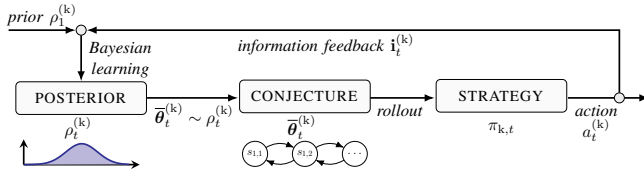


[Fig. 8](#): Conjectural Online Learning (COL); the figure illustrates a time step during which player k updates its conjecture $\bar{\theta}_t^{(k)}$ and its strategy $\pi_{k,t}$.

At time t , player k updates its base strategy $\pi_{k,1}$ as follows¹.

$$\pi_{k,t}(\mathbf{b}_t) \in \mathcal{R}(\bar{\theta}_t^{(k)}, \mathbf{b}_t, \bar{J}_k^{(\pi_t)}, \ell_k) \triangleq \arg \min_{a_t^{(k)}, a_{t+1}^{(k)}, \dots, a_{t+\ell_k-1}^{(k)}} \quad (13)$$

$$\mathbb{E}_{\pi_t} \left[\sum_{j=t}^{t+\ell_k-1} \gamma^{j-t} c_k(S_j, A_j^{(D)}) + \gamma^{\ell_k} \bar{J}_k^{(\pi_t)}(\mathbf{B}_{t+\ell_k}) \mid \mathbf{b}_t \right],$$

where ℓ_k is the lookahead horizon, \mathcal{R} is the rollout operator, $c_D \triangleq c$ ([7](#)), $c_A \triangleq -c$, $\pi_t = (\pi_{k,1}, \bar{\pi}_{-k,t})$, $\bar{J}_k^{(\pi_t)}$ is the cost function induced by $\bar{\theta}_t^{(k)}$ (line 19 in [Alg. 1](#)), and $\bar{\pi}_{-k,t}$ is the conjectured strategy of the opponent (lines 14–17 in [Alg. 1](#)).

The Bellman equation in (13) corresponds to one step of policy iteration with the base strategy as the starting point [[59](#), Eqs. 6.4.1–22]. The effect of $\ell_k > 1$ is that the starting point is moved closer to the **best response** strategy through $\ell_k - 1$ value iterations [[59](#), Eq. 6.3.2–4] [[14](#)]. Hence, the computational complexity of (13) grows exponentially with ℓ_k , as shown in [Fig. 10](#) [[14](#)]. To manage this complexity for large instantiations of Γ_{θ_t} , we estimate \mathbb{E} in (13) using Monte-Carlo samples [[14](#)].

Remark 1. (13) computes the next action as if the conjectures were true, i.e., the action is computed based on (enforced) certainty equivalence [[14](#), p. 185][[48](#), p. 232].

We know from dynamic programming that $\pi_{k,t}$ (13) improves on the base strategy $\pi_{k,1}$ [[60](#), Prop. 1]. The extent of the improvement depends on the lookahead horizon and the accuracy of the conjectures as follows.

Theorem 3. The conjectured cost of player k 's rollout strategy $\pi_{k,t}$ satisfies

$$\bar{J}_k^{(\pi_{k,t}, \bar{\pi}_{-k,t})}(\mathbf{b}) \leq \bar{J}_k^{(\pi_{k,1}, \bar{\pi}_{-k,t})}(\mathbf{b}) \quad \forall \mathbf{b} \in \mathcal{B}. \quad (14a)$$

¹ J_A depends on s , but this dependence is omitted for notational clarity.

Assuming $(\bar{\theta}_t^{(k)}, \bar{\ell}_{-k})$ predicts the game ℓ_k steps ahead, then

$$\|\bar{J}_k^{(\pi_{k,t}, \bar{\pi}_{-k,t})} - J_k^*\| \leq \frac{2\gamma^{\ell_k}}{1-\gamma} \|\bar{J}_k^{(\pi_{k,1}, \bar{\pi}_{-k,t})} - J_k^*\|, \quad (14b)$$

where J_k^* is the optimal cost-to-go function when facing $\pi_{-k,t}$ and $\|J\| \triangleq \max_x |J(x)|$.

[Theorem 3](#) states that the performance bound improves superlinearly when the lookahead horizon ℓ_k increases or when the conjectured cost function \bar{J}_k moves closer to J_k^* ([9](#)), as shown in [Fig. 9](#). In particular, (14b) suggests that ℓ_k controls the trade-off between computational cost and rollout performance; see [Fig. 10](#). We provide proof in [Appendix B](#).

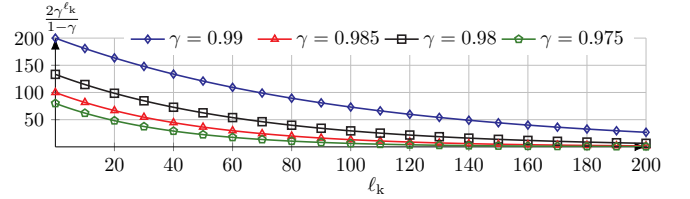
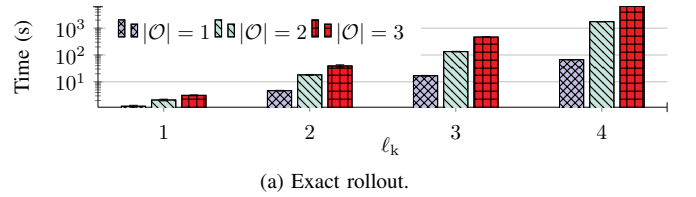
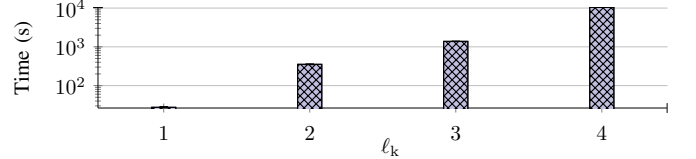


[Fig. 9](#): Illustration of [Thm. 3](#); the x-axis indicates the lookahead horizon ℓ_k ; the y-axis indicates the factor of the performance bound in (14b); the curves relate to different discount factors γ .



(a) Exact rollout.



(b) Monte-Carlo rollout with $|\mathcal{O}| = 26178$.

[Fig. 10](#): Compute time of rollout (13) for varying lookahead horizons ℓ_k and observation space sizes $|\mathcal{O}|$; see [Appendix F](#) for hyperparameters.

After computing (13) and executing the corresponding action, player k receives the feedback $\mathbf{i}_t^{(k)}$ ([3](#)) and updates its conjectures as $\bar{\theta}_t^{(k)} \sim \rho_t^{(k)}$ and $\bar{\ell}_{A,t} \sim \mu_t$ (line 14 in [Alg. 1](#)), where $\rho_t^{(k)}$ and μ_t are adapted through *Bayesian learning* as

$$\rho_t^{(k)}(\bar{\theta}_t^{(k)}) \triangleq \frac{\mathbb{P}[\mathbf{i}_t^{(k)} \mid \bar{\theta}_t^{(k)}, \mathbf{b}_{t-1}] \rho_{t-1}^{(k)}(\bar{\theta}_{t-1}^{(k)})}{\int_{\Theta_k} \mathbb{P}[\mathbf{i}_t^{(k)} \mid \bar{\theta}_t^{(k)}, \mathbf{b}_{t-1}] \rho_{t-1}^{(k)}(d\bar{\theta}_t^{(k)})} \quad (15a)$$

$$\mu_t(\bar{\ell}_A) \triangleq \frac{\mathbb{P}[\mathbf{i}_t^{(D)} \mid \bar{\ell}_A, \mathbf{b}_{t-1}] \mu_{t-1}(\bar{\ell}_A)}{\sum_{\bar{\ell}_A \in \mathcal{L}} \mathbb{P}[\mathbf{i}_t^{(D)} \mid \bar{\ell}_A, \mathbf{b}_{t-1}] \mu_{t-1}(\bar{\ell}_A)}. \quad (15b)$$

These updates are well-defined under this assumption.

Assumption 1. (i) \mathcal{L} is finite and Θ_k is a compact subset of an Euclidean space; (ii) $\rho_1^{(k)}$ and μ_1 have full support; and (iii) for all feasible $(\mathbf{i}^{(k)}, \mathbf{b})$, there exists $\bar{\theta} \in \Theta_k$ and $\bar{\ell}_A \in \mathcal{L}$ that assign positive probability to $\mathbf{i}^{(k)}$ in \mathbf{b} .

Algorithm 1: Conjectural Online Learning.

```

1 Input: Initial belief  $\mathbf{b}_1$ , game model  $\Gamma_{\theta_1}$ ,
2 base strategies  $\pi_1 \triangleq (\pi_{D,1}, \pi_{A,1})$ , priors  $(\mu_1, \rho_1^{(D)}, \rho_1^{(A)})$ ,
3 discount factor  $\gamma$ , lookahead horizons  $\ell_D, \ell_A$ .
4 Output: A sequence of action profiles  $\mathbf{a}_1, \mathbf{a}_2, \dots$ 
5 Algorithm
6   /* Initialization */
7    $\mathbf{h}_1^{(D)} \leftarrow (\mathbf{b}_1), \mathbf{h}_1^{(A)} \leftarrow (\mathbf{b}_1),$ 
8    $s_1 \sim \mathbf{b}_1$ 
9    $\bar{\pi}_{A,1} \leftarrow \pi_{A,1}, \bar{\pi}_{D,1} \leftarrow \pi_{D,1}$ 
10   $a_1^{(D)} \sim \pi_{D,1}(\mathbf{b}_1), a_1^{(A)} \sim \pi_{A,1}(\mathbf{b}_1, s_1)$ 
11   $s_2 \sim f(\cdot | s_1, (a_1^{(D)}, a_1^{(A)}))$ 
12  for  $t = 2, 3, \dots$  do
13    /* Defender learning */
14     $o_t \sim z(\cdot | s_t)$ 
15     $\mathbf{i}_t^{(D)} \leftarrow (o_t), \mathbf{h}_t^{(D)} \leftarrow (\mathbf{h}_{t-1}^{(D)}, \mathbf{i}_t^{(D)}, a_{t-1}^{(D)})$ 
16    Update  $\rho_t^{(D)}$  and  $\mu_t$  (15) and set  $\bar{\theta}_t^{(D)} \sim \rho_t^{(D)}$  and  $\bar{\ell}_{A,t} \sim \mu_t$ 
17     $\mathbf{b}_t \leftarrow \mathbb{B}(\mathbf{h}_t^{(D)}, \bar{\pi}_{A,t-1})$ 
18    Estimate  $\bar{J}_A^{(\pi_{D,t-1}, \pi_{A,1})}$  using  $\Gamma_{\bar{\theta}_t^{(D)}}$ 
19    Compute  $\bar{\pi}_{A,t}(\mathbf{b}_t) \in \mathcal{B}(\bar{\theta}_t^{(D)}, \mathbf{b}_t, \bar{J}_A^{(\pi_{D,t-1}, \pi_{A,1})}, \bar{\ell}_{A,t})$ 
20    Estimate  $\bar{J}_D^{(\pi_{D,1}, \bar{\pi}_{A,t})}$  using  $\Gamma_{\bar{\theta}_t^{(D)}}$ 
21     $\pi_{D,t}(\mathbf{b}_t) \in \mathcal{B}(\bar{\theta}_t^{(D)}, \mathbf{b}_t, \bar{J}_D^{(\pi_{D,1}, \bar{\pi}_{A,t})}, \ell_D)$ 
22    /* Attacker learning */
23     $\mathbf{i}_t^{(A)} \leftarrow (o_t, s_t, a_{t-1}^{(D)}), \mathbf{h}_t^{(A)} \leftarrow (\mathbf{h}_{t-1}^{(A)}, \mathbf{i}_t^{(A)}, a_{t-1}^{(A)})$ 
24    Update  $\rho_t^{(A)}$  using (15a) and set  $\bar{\theta}_t^{(A)} \sim \rho_t^{(A)}$ 
25    Estimate  $\bar{J}_A^{(\pi_{A,1}, \pi_{D,t})}$  using  $\Gamma_{\bar{\theta}_t^{(A)}}$ 
26     $\pi_{A,t}(\mathbf{b}_t) \in \mathcal{B}(\bar{\theta}_t^{(A)}, \mathbf{b}_t, \bar{J}_A^{(\pi_{A,1}, \pi_{D,t})}, \ell_A)$ 
27     $a_t^{(D)} \sim \pi_{D,t}(\mathbf{b}_t), a_t^{(A)} \sim \pi_{A,t}(\mathbf{b}_t, s_t)$ 
28     $s_{t+1} \sim f(\cdot | s_t, (a_t^{(D)}, a_t^{(A)}))$ 
29  end

```

A. Convergence and Equilibrium Analysis

When player k updates its conjectures through (15), the goal is to minimize the *discrepancy* between the feedback distributions induced by the conjectures and the observed feedback (3). We define this discrepancy as

$$K(\bar{\alpha}, \nu) \triangleq \mathbb{E}_{\mathbf{b} \sim \nu} \mathbb{E}_{\mathbf{I}^{(k)}} \left[\ln \left(\frac{\mathbb{P}[\mathbf{I}^{(k)} | \alpha, \mathbf{b}]}{\mathbb{P}[\mathbf{I}^{(k)} | \bar{\alpha}, \mathbf{b}]} \right) | \alpha, \mathbf{b} \right], \quad (16)$$

where $\alpha \in \{\theta, \ell_A\}$ and $\nu \in \Delta(\mathcal{B})$ is an occupancy measure. We say that conjectures that minimize (16) are *consistent* with ν [61]². Hence, the sets of consistent conjectures at time t are

$$\bar{\theta}_t^{(k)} \in \Theta_k^*(\nu_t) \triangleq \arg \min_{\bar{\theta}_t^{(k)} \in \Theta_k} K(\bar{\theta}_t^{(k)}, \nu_t) \quad (17a)$$

$$\bar{\ell}_{A,t} \in \mathcal{L}^*(\nu_t) \triangleq \arg \min_{\bar{\ell}_{A,t} \in \mathcal{L}} K(\bar{\ell}_{A,t}, \nu_t), \quad (17b)$$

where $\nu_t(\mathbf{b}) \triangleq \frac{1}{t} \sum_{\tau=1}^t \mathbb{1}_{\mathbf{b}=\mathbf{b}_\tau}$ is the empirical occupancy measure and $\pi_{\mathbf{h}_t}$ is the empirical strategy profile at time t .

Intuitively, Θ_k^* and \mathcal{L}^* contain the conjectures that player k considers possible after observing feedback generated by ν_t and $\pi_{\mathbf{h}_t}$ [62]. A desirable property of the conjecture distributions (15) is, therefore, that they concentrate on Θ_k^* and \mathcal{L}^* (17). This property is guaranteed asymptotically under the following conditions.

Assumption 2 (Regularity). *For fixed values of $\mathbf{i}^{(k)}$ and θ ,*

²We use the standard convention that $-\ln 0 = \infty$ and $0 \ln 0 = 0$.

- 1) *The mapping $\mathbf{b} \mapsto \ln \mathbb{P}[\mathbf{i}^{(k)} | \theta, \mathbf{b}]$ is Lipschitz w.r.t. the Wasserstein-1 distance, and the Lipschitz constant is independent of $\mathbf{i}^{(k)}$ and θ .*
- 2) *The mapping $\theta \mapsto \ln \mathbb{P}[\mathbf{i}^{(k)} | \theta, \mathbf{b}]$ is continuous and there exists an integrable function $g_{\mathbf{b}}(\mathbf{i}^{(k)})$ for all $\mathbf{b} \in \mathcal{B}$ such that $|\ln \frac{\mathbb{P}[\mathbf{i}^{(k)} | \theta, \mathbf{b}]}{\mathbb{P}[\mathbf{i}^{(k)} | \bar{\theta}, \mathbf{b}]}| \leq g_{\mathbf{b}}(\mathbf{i}^{(k)})$ for all $\bar{\theta} \in \Theta_k$.*

Theorem 4. *Given Assumptions 1–2, the following holds for any sequence $(\pi_{\mathbf{h}_t}, \nu_t)_{t \geq 1}$ generated by COL.*

$$\lim_{t \rightarrow \infty} \sum_{\bar{\ell}_A \in \mathcal{L}} (K(\bar{\ell}_A, \nu_t) - K_{\mathcal{L}}^*(\nu_t)) \mu_{t+1}(\bar{\ell}_A) = 0 \quad (\text{A})$$

a.s. - $\mathbb{P}^{\mathcal{H}}$, and provided that $\theta_t = \theta_1$ for all t ,

$$\lim_{t \rightarrow \infty} \int_{\Theta_k} (K(\bar{\theta}, \nu_t) - K_{\Theta_k}^*(\nu_t)) \rho_{t+1}^{(k)}(d\bar{\theta}) = 0 \quad (\text{B})$$

a.s. - $\mathbb{P}^{\mathcal{H}}$, where $(K_{\mathcal{L}}^, K_{\Theta_k}^*)$ denote the minimal values of (17) and $\mathbb{P}^{\mathcal{H}}$ is a probability measure over the set of realizable histories $\times_{t \geq 1} (\mathcal{H}_t^{(D)} \times \mathcal{H}_t^{(A)})$ that is induced by $(\pi_{\mathbf{h}_t})_{t \geq 1}$.*

Theorem 4 states that the conjectures produced by COL are asymptotically consistent (17) (see Appendices C–D for the proof). This consistency means that if the sequence $(\pi_{\mathbf{h}_t}, \nu_t)_{t \geq 1}$ generated by COL converges, then it converges to an equilibrium of the following form.

Definition 2 (Berk-Nash equilibrium, adapted from [63]). *$(\pi, \nu) \in \Pi \times \Delta(\mathcal{B})$ is a Berk-Nash equilibrium of Γ_{θ_t} (Prob. 1, COL) iff there exist a $\rho^{(k)} \in \Delta(\Theta_k)$ for each player $k \in \{D, A\}$ such that*

- (i) **BOUNDED RATIONALITY.** π_k is a *best response* against π_{-k} for any \mathbf{b} given $(\nu, \rho^{(k)}, \rho^{(-k)})$, (ℓ_k, ℓ_{-k}) , and π_1 .
- (ii) **CONSISTENCY.** $\rho^{(k)} \in \Delta(\Theta_k^*(\nu))$.
- (iii) **STATIONARITY.** (π, ν) is a limit point of some sequence $(\pi_{\mathbf{h}_t}, \nu_t)_{t \geq 1}$ generated by COL, satisfying

$$\nu(\mathbf{b}') = \int_{\mathcal{B}} \mathbb{E}_{A^{(D)}, O, \Gamma_{\hat{\theta}}} [\delta_{\mathbf{b}'}(\mathbb{B}(\mathbf{b}, A^{(D)}, O, \pi_A))] d\nu(\mathbf{b}),$$

where \mathbb{B} is the belief operator defined in (6) and $\Gamma_{\hat{\theta}}$ is parameterized by $\hat{\theta} \triangleq \int_{\Theta_D} \bar{\theta} d\rho^{(D)}(\bar{\theta})$.

Corollary 1 (Berk-Nash is a fixed point of COL).

- (A) *If the sequence $(\pi_{\mathbf{h}_t}, \nu_t)_{t \geq 1}$ generated by COL converges to (π, ν) , then (π, ν) is a Berk-Nash equilibrium.*
- (B) *Given a Berk-Nash equilibrium (π, ν) and assuming*

$$\bar{\theta}^{(k)} \in \Theta_k^*(\nu) \implies \mathbb{P}[\mathbf{I}^{(k)} | \bar{\theta}^{(k)}, \mathbf{b}] = \mathbb{P}[\mathbf{I}^{(k)} | \theta, \mathbf{b}] \quad (18a)$$

$$\ell_D = \ell_A = \infty, \quad (18b)$$

then (π, \mathbb{B}) is a perfect Bayesian equilibrium.

Proof. Condition (i) in Def. 2 is ensured by rollout (13); condition (ii) is ensured asymptotically by Thm. 4; and condition (iii) is a consequence of convergence. Hence, statement (A) holds. Now consider statement (B). Condition 2) in Def. 1 is satisfied by definition of \mathbb{B} (6). To see why condition 1) also must hold, note that assumption (18a) together with condition (ii) of Def. 2 implies that $\mathbb{P}[\mathbf{I}^{(k)} | \theta, \mathbf{b}] = \mathbb{P}[\mathbf{I}^{(k)} | \bar{\theta}^{(k)}, \mathbf{b}]$ for any $\bar{\theta}^{(k)} \sim \rho^{(k)}$. Consequently, it follows from assumption (18b) that $\pi_A \in \mathcal{B}_A(\pi_D)$ and $\pi_D \in \mathcal{B}_D(\pi_A)$ for any \mathbf{b}_1 (9). \square

Corollary 1 states that if the sequence $(\pi_{h_t}, \nu_t)_{t \geq 1}$ generated by COL converges, then it must converge to a **Berk-Nash equilibrium**. Further, under the conditions defined in (18), this equilibrium is also a **perfect Bayesian equilibrium**. The converse is not necessarily true, however, since the **perfect Bayesian equilibrium** does not enforce condition (iii) of the **Berk-Nash equilibrium**. This condition requires that ν_t converges to a stationary distribution, which is not guaranteed to exist. We provide an example in Appendix E. Whether a stationary distribution exists or not depends primarily on the parameter vector θ_t and the observation function z (4).

VI. DIGITAL TWIN AND SYSTEM IDENTIFICATION

To implement and evaluate the method described above for the APT use case (§II), we estimate the parameters of Γ (1) using a digital twin of the target infrastructure.

A. Creating a Digital Twin of the Target Infrastructure

The configuration of the target infrastructure is listed in Appendix G. The topology is shown in Fig. 1. It consists of $N = 64$ servers, some of which are vulnerable to APTs.

We create a digital twin of the target infrastructure using an open-source emulation system, which is based on Linux containers and emulates network connectivity with Linux bridges [40]; see Fig. 11. The containers run software functions replicating important components of the target infrastructure, such as web servers, vulnerabilities, and the SNORT IDPS (ruleset v2.9.17.1). We implement network isolation and traffic shaping using network namespaces and the NETEM module in the Linux kernel [64]. Resource allocation to containers, e.g., CPU and memory, is enforced using CGROUPS. We emulate the attacker using the actions in Table 2. Similarly, we emulate the defender through hypervisor-based recovery of servers and blocking of IP addresses using a firewall [65]. Software programs implementing these actions are available at [40].

B. Estimating the Observation Distribution

Following the APT use case described in §II, we define the observation o_t (4) to be the priority-weighted sum of the number of IDS alerts at time t . For the evaluation reported in this paper, we collect about $M = 10^5$ measurements of o_t in the digital twin (the measurements are available at [40], where $|\mathcal{O}| = 26178$). Using these measurements, we estimate the observation distribution z (4) with the empirical distribution \hat{z} , where $\hat{z} \xrightarrow{a.s.} z$ as $M \rightarrow \infty$ (Glivenko-Cantelli theorem).

VII. EXPERIMENTAL EVALUATION OF COL

We implement COL (Fig. 8, Alg. 1) in Python and evaluate it through simulation and emulation studies based on the digital twin (Fig. 11). The source code of our implementation is available at [40]. The simulation environment and the digital twin runs on a server with a 24-core INTEL XEON GOLD 2.10 GHz CPU and 768 GB RAM. Hyperparameters for COL and Γ (1) are listed in Appendix F.

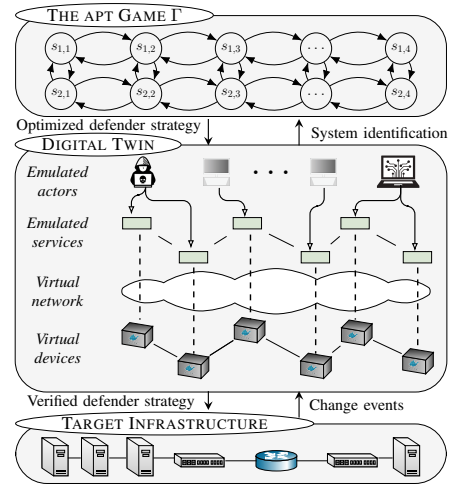


Fig. 11: The digital twin is a virtual replica of the target infrastructure; we use the twin for evaluation and data collection [40].

Type	Actions	MITRE ATT&CK technique
Reconnaissance	TCP SYN scan, UDP scan	T1046 service scanning
	TCP XMAS scan	T1046 service scanning
	VULSCAN	T1595 active scanning
	ping-scan	T1018 system discovery
		T1110 brute force
Brute-force	TELNET, SSH	T1110 brute force
	FTP, CASSANDRA	T1110 brute force
	IRC, MONGODB, MYSQL	T1110 brute force
	SMTTP, POSTGRES	T1110 brute force
		T1210 service exploitation
Exploit	CVE-2017-7494	T1210 service exploitation
	CVE-2015-3306	T1210 service exploitation
	CVE-2010-0426	T1068 privilege escalation
	CVE-2015-5602	T1068 privilege escalation
	CVE-2015-1427	T1210 service exploitation
	CVE-2014-6271	T1210 service exploitation
	CVE-2016-10033	T1210 service exploitation
	SQL injection (CWE-89)	T1210 service exploitation

TABLE 2: Attacker actions on the digital twin (§II); when the attacker takes the stop action (§III-A), a randomly selected action is applied to every reachable server; actions are identified by the vulnerability identifiers in the Common Vulnerabilities and Exposures (CVE) database [66] and the Common Weakness Enumeration (CWE) list [67]; the actions are also linked to the corresponding attack techniques in MITRE ATT&CK [68].

A. Evaluation Scenarios

We define five scenarios to evaluate the performance properties of COL (Fig. 8, Alg. 1). The first four scenarios are evaluated in simulation, and the fifth scenario is evaluated on the digital twin. Our aim in evaluating these scenarios is to assess a) the computational requirements of rollout (13); b) the convergence rate of COL for different instantiations of Γ_{θ_t} (Prob. 1); and c), the benefit of COL compared to existing intrusion response systems.

Each evaluation scenario is based on an instantiation of Prob. 1 for the APT use case (§II) with the model described in §III. In such an instantiation, the defender and the attacker take actions at time steps $t = 1, 2, \dots$. During each step, they perform one action each: either a (passive) *continue* action or a *stop action* (see §III-A). The defender’s stop action corresponds to hypervisor-based recovery of servers (scenarios 1–4) or blocking of IP addresses (scenario 5) [65]. The attacker’s stop action is drawn randomly from Table 2.

After executing the actions, the observations are either sampled from the estimated observation distribution (scenarios 1–4) or measured directly from the digital twin (scenario 5). The main difference between the evaluation scenarios is how the attacker and the defender models are misspecified, as explained below.

Scenario 1 (Defender is uncertain about ℓ_A). In this scenario, the game is stationary (i.e., $\theta_t = \theta_1$ for all t). θ_1 represents the complete game model (1) and is known to both players (i.e., $\rho_1^{(k)}(\theta_1) = 1$), but the defender is uncertain about the attacker’s computational capacity ℓ_A , i.e., $\mu_1(\ell_A) < 1$.

Scenario 2 (Non-stationary θ_t). In this scenario, ℓ_A is known to the defender, but the game is non-stationary, and z (4) is parameterized by θ_t , which represents the number of clients. Hence, θ_t changes whenever a client arrives or departs. Clients have exponential service times and arrive following a Poisson process with the following rate function (see Figs. 12–13) [69]

$$\lambda(t) = \exp\left(\underbrace{\sum_{i=1}^{\dim(\psi)} \psi_i t^i}_{\text{trend}} + \underbrace{\sum_{k=1}^{\dim(\chi)} \chi_k \sin(\omega_k t + \phi_k)}_{\text{periodic}}\right). \quad (19)$$

See Appendix F for the parameter values.

Scenario 3 (Misspecified model conjectures $\rho_t^{(D)}, \rho_t^{(A)}$). In this scenario, the game is stationary (i.e., $\theta_t = \theta_1$ for all t) and θ_1 represents the compromise probability p_A (2). Further, the attacker’s computational capacity ℓ_A is known to the defender, but both players are uncertain about θ_1 and have misspecified conjectures, i.e., $\theta_1 \notin \Theta_A \cup \Theta_D$.

Scenario 4 (Defender is uncertain about ℓ_A and θ_t). This scenario is the same as Scenario 3, except that the defender is uncertain about ℓ_A , i.e., $\mu_1(\ell_A) < 1$.

Scenario 5 (Comparison with the SNORT IDPS [41]). In this scenario, we compare COL with the SNORT IDPS (ruleset v2.9.17.1). We use two baselines: SNORT-HIGH and SNORT-MEDIUM, which block IP traffic that generates alerts with high and medium priority, respectively. The attacker follows the fixed strategy $\pi_A(S | \cdot) = 1$ and spoofs its IP address. The observation o_t (4) represents a SNORT alert, where $o_t = 0$ means no alert. The defender’s response action (§III-A) corresponds to blocking the IP address that generated the alert. θ_t parameterizes z (4) and represents the distributions of alert priorities generated by the clients and the attacker. Specifically, $\Theta_D = \{\theta', \theta''\}$ and

$$\theta' \triangleq \begin{matrix} & \text{C} & \text{A} \\ \text{N} & \begin{bmatrix} 0.85 & 0.4 \end{bmatrix} \\ \text{M} & \begin{bmatrix} 0.1 & 0.3 \end{bmatrix} \\ \text{H} & \begin{bmatrix} 0.05 & 0.3 \end{bmatrix} \end{matrix} \quad \theta'' \triangleq \begin{matrix} & \text{C} & \text{A} \\ \text{N} & \begin{bmatrix} 0.4 & 0.1 \end{bmatrix} \\ \text{M} & \begin{bmatrix} 0.3 & 0.1 \end{bmatrix} \\ \text{H} & \begin{bmatrix} 0.3 & 0.8 \end{bmatrix} \end{matrix}, \quad (20)$$

where $\theta_t = \theta'$ for $t < 50$ and $\theta_t = \theta''$ for $t \geq 50$. Here, N, M, and H refer to no alert, medium priority alert, and high priority alert, respectively. Similarly, C and A refer to the client and the attacker, respectively.

Remark 2. In practice, the prior over θ_1 for the instantiations described above can be defined based on domain knowledge

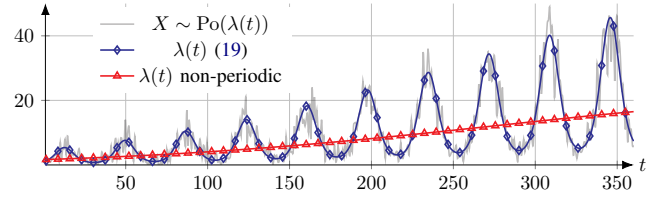


Fig. 12: The arrival rate function (19) used in Scenario 2; the blue curve shows the arrival rate $\lambda(t)$; the red curve shows the trend of $\lambda(t)$ without the periodic effects; and the shaded black curve shows the number of arrivals.

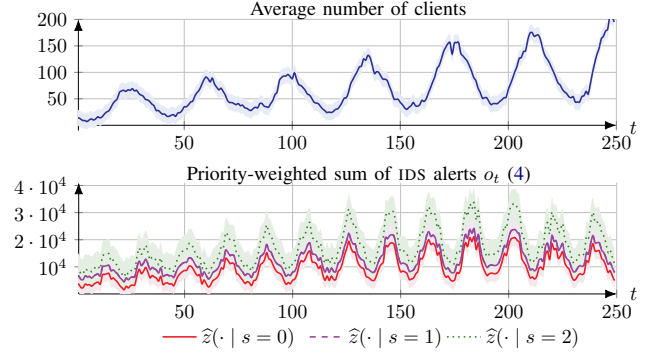


Fig. 13: Estimated distributions of the number of clients and the priority-weighted sum of IDS alerts o_t (4) during different arrival rates $\lambda(t)$ (19) based on the APT actions listed in Table 2 and the rate function shown in Fig. 12; the curves indicate mean values and the shaded areas indicate standard deviations from 3 measurements; the measurements are available at [40].

or obtained through system measurements. Companies like Google, Meta, and IBM have documented procedures for estimating such distributions [70]. Similarly, the prior over ℓ_k can be obtained from opponent modeling [71].

B. Evaluation Results (Figs. 14–16, Table 3)

Scenario 1. Figure 14.a–b show the evolution of the conjecture distribution μ_t (15b) and the discrepancy (16) of the conjecture $\bar{\ell}_{A,t}$ when $\mathcal{L} = \{1, 2\}$ and $\ell_A = 1$. We observe that μ_t converges and concentrates on the consistent conjecture (17) after 5 time steps, as predicted by Thm. 4.A. Figure 14.d shows the rate of convergence for different $|\mathcal{L}|$, indicating that a larger $|\mathcal{L}|$ leads to a slower convergence. This is expected since a larger $|\mathcal{L}|$ means the defender has more uncertainty about ℓ_A .

Figure 14.c shows the expected cost of the defender as a function of $|\ell_A - \bar{\ell}_{A,t}|$, which quantifies the inaccuracy of the defender’s conjecture $\bar{\ell}_{A,t}$. We observe that the defender’s cost is increasing with the inaccuracy of its conjecture. Next, Fig. 14.e shows the evolution of the discrepancy (16) of different conjectures. We observe that the discrepancies of the incorrect conjectures increase over time and that the discrepancy of the correct conjecture is 0 (by definition).

Lastly, Fig. 14.f shows the expected cost of COL and the expected cost of best response reinforcement learning with CEM [50] (i.e., best response dynamics [72]). We note that the expected cost of reinforcement learning oscillates. Similar behavior of reinforcement learning has been observed in related work [30], [73]. The oscillation indicates that the players alternate between different best responses in a cycle.

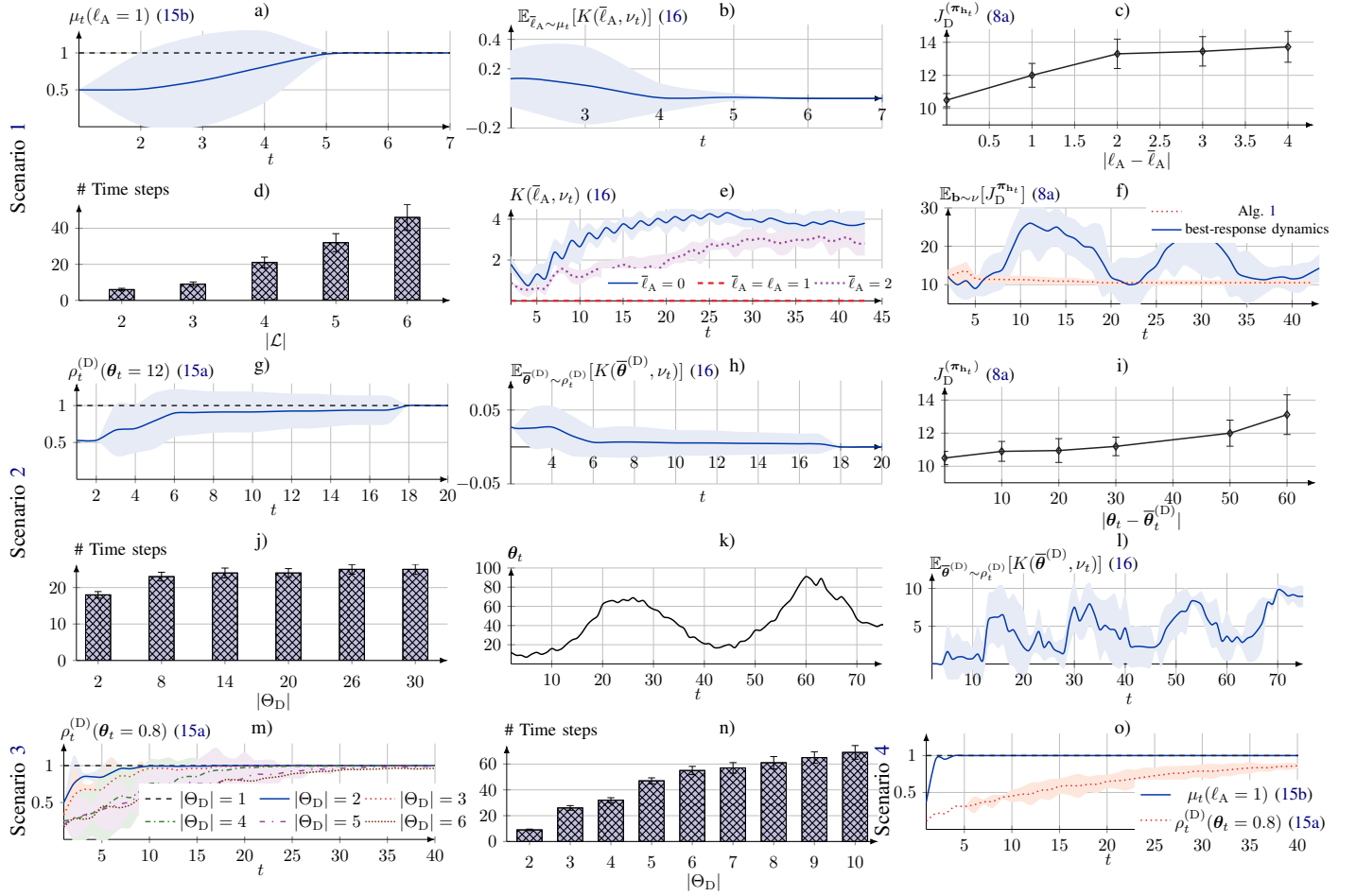


Fig. 14: Evaluation results; a)–f) relate to **Scenario 1**; g)–l) relate to **Scenario 2**; m)–n) relate to **Scenario 3**; and o) relate to **Scenario 4**; values indicate the mean; the shaded areas and the error bars indicate the 95% confidence interval based on 20 random seeds; hyperparameters are listed in [Appendix F](#).

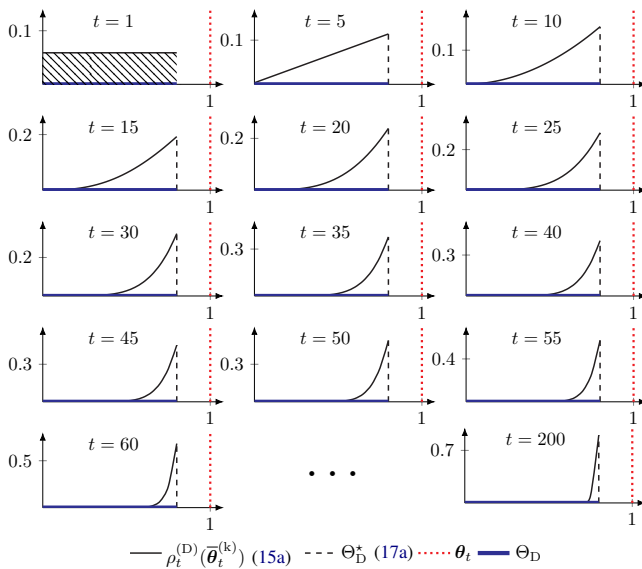


Fig. 15: Evolution of $\rho_t^{(D)}$ (15a) when $\Theta_D = \{0.0, 0.05, \dots, 0.8\}$ and $\theta_t = 1$ for all t (**Scenario 3**); hyperparameters are listed in [Appendix F](#).

By contrast, the expected cost of COL is significantly more stable, and its behavior is consistent with convergence to a **Berk-Nash equilibrium**. The strategy oscillations induced by reinforcement learning lead to unpredictability, making it an impractical solution for operational systems. In comparison, the **Berk-Nash equilibrium** provides a robust and reliable strategy for the defender; see [Fig. 14.f](#).

Scenario 2. Figures 14.g–h show the evolution of the defender’s conjecture distribution $\rho_t^{(D)}$ (15a) and the discrepancy (16) of the conjecture $\bar{\theta}_t^{(D)}$ when $\Theta_D = \{12, 9\}$ and $\theta_t = 12$ for all t . We observe that $\rho_t^{(D)}$ converges and concentrates on the consistent conjecture (17) after 18 time steps, as predicted by [Thm. 4.B](#). [Figure 14.j](#) shows the rate of convergence for varying $|\Theta_D|$. As expected, when the defender’s uncertainty about θ_t increases (i.e., when $|\Theta_D|$ increases), the time it takes for the sequence of conjectures to converge increases.

[Figure 14.i](#) shows the defender’s cost as a function of $|\theta_t - \bar{\theta}_t^{(D)}|$, which quantifies the inaccuracy of the defender’s conjecture $\bar{\theta}_t^{(D)}$. We observe that the cost is increasing with the inaccuracy of the conjecture. Lastly, [Figs. 14.k–l](#) show the expected discrepancy (16) of the posterior (15a) when θ_t is changing at every time step, whereby $\rho_t^{(D)}$ does not converge. (Note that [Thm. 4](#) only applies when θ_t remains fixed.)

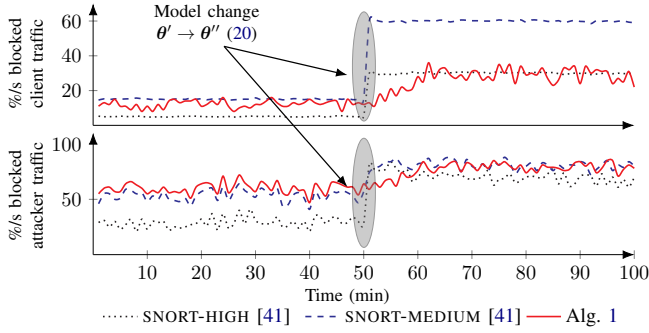


Fig. 16: Scenario 5: percentage of blocked network traffic in the digital twin.

Scenario 3. Figures 14.m–n show the time for the defender’s conjecture $\bar{\theta}_t^{(D)}$ to converge for different sizes of Θ_D when θ_t is fixed. We observe that the time to converge increases with the size of Θ_D , which is expected since the size of Θ_D represents the defender’s degree of uncertainty about θ_t . Figure 15 shows the evolution of $\rho_t^{(D)}$. We observe that $\rho_t^{(D)}$ starts from a uniform distribution over Θ_D and as $t \rightarrow \infty$, it concentrates on the set of consistent conjectures Θ_D^* (17a).

Scenario 4. Figure 14.o shows the evolution of the defender’s conjecture distributions μ_t and $\rho_t^{(D)}$ (15). We observe that both distributions converge, which is consistent with Thm. 4. The convergence of μ_t is significantly faster than that of $\rho_t^{(D)}$. We believe this difference is because $|\mathcal{L}| < |\Theta_D|$, which means that the defender is more uncertain about ℓ_A than about θ_t .

Scenario 5. Figure 16 shows the percentage of blocked attacker and client traffic when running the SNORT IDPS [41] and COL on the digital twin. We observe that both block some client traffic and fail to block some attacker traffic, which is expected considering the false IDS alarms generated by the clients. When comparing COL with SNORT we find that a) COL and IPS-HIGH blocks the least *client* traffic; and b) IPS-MEDIUM and COL blocks the most *attacker* traffic. This suggests to us that COL balances the trade-off between blocking clients and the attacker based on the cost function (7). Further, COL adapts when θ_t changes.

Comparison with state-of-the-art methods. The convergence times of COL and methods used in prior work are listed in Table 3. While we observe that COL converges faster than the baselines, a direct comparison is not feasible for two reasons. First, the baselines do not consider the same solution concept as us, i.e., the Berk-Nash equilibrium (Def. 2). Second, the baselines make different assumptions about the computational capacity and information available to the players. For example, fictitious play [74], which is a popular method among prior work, assumes that players a) have correctly specified models and b) have unlimited computational capacity. Similarly, reinforcement learning methods like PPO [75, Alg. 1] and NFSP [76, Alg. 9] are designed for offline rather than online learning.

C. Discussion of the Evaluation Results

The experimental findings can be summarized as follows.

Method	Fixed point	Time (min)
COL, $ \mathcal{L} = 2, \Theta_k = 1$	Berk-Nash equilibrium	6.7 ± 0.7
COL, $ \mathcal{L} = 3, \Theta_k = 1$	Berk-Nash equilibrium	11.4 ± 0.9
COL, $ \mathcal{L} = 4, \Theta_k = 1$	Berk-Nash equilibrium	39.1 ± 1.3
COL, $ \mathcal{L} = 8, \Theta_k = 1$	Berk-Nash equilibrium	137.3 ± 2.8
COL, $ \mathcal{L} = 1, \Theta_k = 2$	Berk-Nash equilibrium	12.9 ± 0.9
COL, $ \mathcal{L} = 1, \Theta_k = 32$	Berk-Nash equilibrium	17.9 ± 1.0
COL, $ \mathcal{L} = 1, \Theta_k = 192$	Berk-Nash equilibrium	29.9 ± 1.2
COL, $ \mathcal{L} = 4, \Theta_k = 192$	Berk-Nash equilibrium	194.6 ± 3.7
Best-response dynamics (Fig. 14.f)	ϵ -Nash equilibrium [51, Eq. 1]	DNC
HSVI [57, Alg. 1] (Fig. 7)	ϵ -Nash equilibrium [51, Eq. 1]	DNC
NFSP [76, Alg. 9]	ϵ -Nash equilibrium [51, Eq. 1]	≈ 919 min
Fictitious play [74]	ϵ -Nash equilibrium [51, Eq. 1]	≈ 4800 min
PPO [75, Alg. 1], static π_A	Best response	9.2 ± 0.4 min

TABLE 3: Comparison with baseline methods in terms of speed of convergence; DNC is short for “does not converge”; “ \approx ” means that the algorithm nearly converges; numbers indicate the mean and the standard deviation from evaluations with 3 random seeds; hyperparameters are listed in Appendix F.

- 🔍 The conjectures produced by COL converge to consistent conjectures once the model parameters θ_t remain fixed (17) (Figs. 14.a,g,m,o, Thm. 4). The rate of convergence decreases as $|\mathcal{L}|$ and $|\Theta_k|$ increase (Figs. 14.d,j,n).
- 🔍 The defender’s cost increases as the distance between its conjecture and the true model increases (Figs. 14.c,i).
- 🔍 COL allows configuring the computational capacity and the uncertainty of each player k by tuning ℓ_k (Fig. 10) and (\mathcal{L}, Θ_k) , respectively (Fig. 14).
- 🔍 COL leads to effective strategies (Thm. 3) that are more stable than those obtained through reinforcement learning (Fig. 14.f, Table 3).
- 🔍 COL outperforms the SNORT IDPS [41] in several key metrics; see Fig. 16.
- 🔍 Computation of perfect Bayesian equilibria and computation of exact rollout strategies is intractable for any non-trivial instantiation of Γ (Fig. 7, Fig. 10a).
- 🔍 Approximate best response and rollout strategies of Γ can be efficiently computed using stochastic approximation (Fig. 10b, Fig. 5, Thm. 1).

The above findings suggest that COL can produce effective security strategies without relying on a correctly specified model of the environment. The practical implication of this result is that COL is suitable for dynamic IT infrastructures with short update cycles, which aligns with current trends of virtualization and zero-touch management.

VIII. RELATED WORK

Since the early 2000s, researchers have studied automated security through modeling attacks and response actions on an IT infrastructure as a game between an attacker and a defender (see textbooks [5], [32], [77] and surveys [78], [79]). The game is modeled in different ways depending on the use case. Examples include: APT games [2], [3], [42], [80], [81], honeypot placement games [6], [7], resource allocation games [82], distributed denial-of-service games [29], [31], jamming games [83], data corruption games [84], moving target defense games [78], [85], and intrusion response games [8], [9], [30], [86]–[89]. These games are formulated using various models from the game-theoretic literature. For example: stochastic games (see e.g., [83], [86], [87], [90]), extensive-form games (see e.g., [32]), Blotto games (see e.g., [82]), hypergames

(see e.g., [25], [26]), POSGs (see e.g., [29], [30]), Stackelberg games (see e.g., [29], [84], [89]), differential games (see e.g., [80], [91]), Bayesian games (see e.g., [31], [32], [42], [92]), and evolutionary games (see e.g., [85], [88]).

The main difference between this paper and the works referenced above is that we propose a method for online learning in non-stationary security games in which players have misspecified game models. By contrast, the referenced works assume that players have correctly specified models.

While the study of learning with misspecified models has attracted long-standing interest in economics [15], engineering [16], and psychology [17], it remains unexplored in the security context. Related research in the security literature includes a) games with imperfect and incomplete information; b) games with bounded rationality; and c) model-free learning approaches. In the following subsections, we describe how these three research areas relate to this paper. The main differences are listed in Table 4.

A. Security Games with Imperfect and Incomplete Information

Security games with imperfect and incomplete information include POSGs [8], [29], [30] and Bayesian games [31], [32], [42], [92]. These games capture scenarios where players have private knowledge represented by *types* or *observations*. Still, the players’ perceptions about how the game works are identical (as defined by a common prior); the only thing distinguishing players is the information each has received [43], [96]. Conversely, our model allows to capture *misspecification*, where players have incorrect *conjectures* about the game’s structure and the opponents’ strategies. Such misspecification encapsulates players’ subjective perception of how the game works and can include both game elements [63] and other players’ strategies [15]. Moreover, players can disagree on the very form of the game. For instance, one player may represent the game with a scalar, whereas another represents it with a high-dimensional vector (see Prob. 1). Such disagreements are captured by the **Berk-Nash equilibrium** but not the **perfect Bayesian equilibrium**.

B. Security Games with Bounded Rationality

The concept of bounded rationality was introduced by Herbert A. Simon in the 1950s as a critique of the assumption of perfect rationality in classical game theory [97]. Research on security games with bounded rationality includes [11], [21]–[23], [25]–[28], [85], [90]. These works differ from this paper in three main ways. First, they do not consider model misspecification as we do in this paper. Second, they study different types of games, i.e., one-stage games [11], [23]; network interdiction games [21]; differential games [28]; Stackelberg games [22]; behavioral games [28]; evolutionary games [85], and hypergames [25], [26]. Third, they study different types of equilibria, i.e., Nash equilibria [27]; Gestalt Nash equilibria [11], [23]; Stackelberg equilibria [21], [22]; evolutionary stable equilibria [85], and hyper Nash equilibria [25], [26]. By contrast, we study **Berk-Nash equilibria** [15, Def. 1] and a POSG where players have misspecified models. The benefit of our game model and equilibrium concept is that they better capture the APT use case (§II).

C. Learning in Security Games

Prior work that studies learning in security games includes [4], [8], [9], [30], [37], [38], [87], [93]–[95]. This paper differs from these works in two main ways. First, we design a novel way to update strategies using rollout with a conjectured model. This contrasts with all of the referenced works which consider other types of strategy updates, e.g., offline learning [8], [9], [95], meta-learning [37], model-free learning [30], [38], [87], [98], [99], and learning with perfect rationality [93], [94]. The advantage of our approach is that it allows us to model players with limited computational capacity and varying degrees of misspecification. Second, we design a convergent Bayesian mechanism for online learning. In comparison, most of the prior work considers other types of learning mechanisms, e.g., fictitious play [8], [9], reinforcement learning [30], [38], [87], [98], [99], online gradient descent [39], and no-regret learning [93], [94].

IX. CONCLUSION AND FUTURE WORK

This paper presents **Conjectural Online Learning (COL)**, a new game-theoretic method for online learning of security strategies that applies to dynamic IT environments where the attacker and defender are uncertain about the environment and the opponent’s strategy. We formulate the interaction between an attacker and a defender as a non-stationary game where each player has a probabilistic conjecture about the game model, which may be misspecified in the sense that the true model has probability 0. Both players iteratively adapt their conjecture using Bayesian learning and update their strategy using rollout. We prove that the conjectures converge to best fits (Thm. 4), and we provide a bound on the performance improvement that rollout enables with a conjectured model (Thm. 3). To characterize the steady state of the game, we propose a novel equilibrium concept based on the **Berk-Nash equilibrium**, which represents a stable point where each player acts optimally given its conjecture (Def. 2). We present **COL** through an APT use case (§II). Evaluations on a testbed show that **COL** produces effective security strategies that adapt to a changing environment (Fig. 14). It also leads to faster convergence than current reinforcement learning techniques and outperforms the SNORT IDPS [41] (Table 3 and Fig. 16).

This paper opens up several directions for future work. One direction is to adapt **COL** to additional use cases. In particular, this paper considers an attacker with inside information – in future work, we plan to investigate use cases with less capable attackers. Another direction of future work is to complement our asymptotic results (Thm. 4) with finite sample bounds and to relate our definition of the **Berk-Nash equilibrium** with other equilibrium concepts. A third direction of future work is to instantiate our game with an observation function (4) that is based on dynamic information flow tracking [44] and to compare rollout with regret minimization [100].

X. ACKNOWLEDGMENTS

The authors would like to thank Branislav Bosanský for sharing the code of the HSVI algorithm.

Paper	Use case	Method	Equilibrium	Evaluation	Game type
[89] Zonouz, 2009	Intrusion response	Dynamic programming	-	Testbed	Stationary POSG
[87] Zhu, 2009	Intrusion detection	Q-learning	Nash	Simulation	Stationary stochastic dynamic game
[93] Balcan, 2015	Resource allocation	No-regret learning	-	Analytical	Stationary repeated Stackelberg game
[94] Lisý, 2016	Resource allocation	No-regret learning	Nash	Analytical	Stationary NFGSS
[11] Chen, 2019	Risk management	Proximal optimization	Gestalt Nash	Simulation	Stationary one-stage game
[21] Sanjab, 2020	Drone operation	Prospect theory	Stackelberg	Simulation	Stationary network interdiction game
[26] Bakker, 2020	Intrusion response	Analytical	Hyper Nash	Simulation	Stationary repeated hypergame
[27] Abdallah, 2020	Power grid	Analytical	Nash	Simulation	Stationary behavioral game
[95] Huang, 2020	APT	Optimization	Perfect Bayes Nash	Simulation	Stationary POSG
[10] Zhao, 2020	Intrusion response	Analytical	Nash	Simulation	Non-stationary Markov game
[31] Aydeger, 2021	DDOS	Optimization	Perfect Bayes Nash	Testbed	Stationary signaling game
[25] Wan, 2022	APT	Analytical	Hyper Nash	Simulation	Stationary hypergame
[22] Gabrys, 2023	Cyber deception	Analytical	Stackelberg	Simulation	Stationary Stackelberg game
[8] Hammar, 2023	Intrusion response	Fictitious play	Nash	Testbed	Stationary POSG
[28] Mavridis, 2023	Cyber-physical security	Stochastic approximation	Nash	Simulation	Stationary differential game
[37] Ge, 2023	Zero-trust	Meta-learning	-	Simulation	Stationary POMDP
This paper, 2025	APT	Bayesian learning & rollout	Berk-Nash	Testbed & simulation	Non-stationary and misspecified POSG

TABLE 4: Comparison between this paper and related work.

APPENDIX A PROOF OF THEOREM 1

Given (π_A, π_D) , the **best response** strategies $(\tilde{\pi}_D, \tilde{\pi}_A)$ are optimal strategies in two POMDPs \mathcal{M}_D^P and \mathcal{M}_A^P . Hence, it suffices to show that there exist optimal strategies π_D^* and π_A^* in \mathcal{M}_D^P and \mathcal{M}_A^P that satisfy (10a) and (10b), respectively. Towards this proof, we state the following five lemmas.

Lemma 1. \mathcal{M}_D^P can be formulated as a repeated optimal stopping problem.

Proof. By definition, an optimal strategy π_D^* in \mathcal{M}_D^P satisfies

$$\begin{aligned}
\pi_D^* &\in \arg \min_{\pi_D \in \Pi_D} \mathbb{E}_{(\pi_D, \pi_A)} \left[\sum_{t=1}^{\infty} \gamma^{t-1} c(S_t, A_t^{(D)}) \mid S_1 = 0 \right] \\
&\stackrel{(a)}{=} \arg \min_{\pi_D \in \Pi_D} \left[\mathbb{E}_{(\pi_D, \pi_A)} \left[\sum_{t=1}^{\tau_1} \gamma^{t-1} c(S_t, A_t^{(D)}) \mid S_1 = 0 \right] + \right. \\
&\quad \left. \mathbb{E}_{(\pi_D, \pi_A)} \left[\sum_{t=\tau_1+1}^{\tau_2} \gamma^{t-1} c(S_t, A_t^{(D)}) \mid S_{\tau_1} = 0 \right] + \dots \right] \\
&= \arg \min_{\pi_D \in \Pi_D} \left[\gamma^{\tau_1} J_D(\mathbf{e}_1) \right. \\
&\quad \left. + \mathbb{E}_{(\pi_D, \pi_A)} \left[\sum_{t=1}^{\tau_1} \gamma^{t-1} c(S_t, A_t^{(D)}) \mid S_1 = 0 \right] \right], \tag{21}
\end{aligned}$$

where τ_1, τ_2, \dots are the stopping times; J_D is the cost-to-go function in \mathcal{M}_D^P (8a); $\mathbf{e}_1 = (1, 0)$; and (a) follows by linearity of \mathbb{E} . Since $\mathbb{E}_{\pi_D} [J_D(\mathbf{e}_1)]$ can be seen as a fixed recovery cost, (21) defines an optimal stopping problem. \square

Lemma 2. The optimal cost-to-go function $J_D^*(\mathbf{b})$ in \mathcal{M}_D^P is piecewise linear and concave with respect to $\mathbf{b} \in \mathcal{B}$.

Proof. Edward J. Sondik originally proved this property [58, Thm. 2]. A more accessible proof can be found in [49, Thms. 7.6.1–7.6.2]. For brevity, we omit it here. \square

Lemma 3. Let $\mathcal{S} \subseteq \mathcal{B}$ denote the subset of the belief space in \mathcal{M}_D^P where it is optimal to stop, i.e., $\mathbf{b} \in \mathcal{S} \iff \pi_D^*(\mathbf{b}) = S$. If $N = 1$, then \mathcal{S} is a convex set [49, Thm. 2.2.1].

Proof. As $N = 1$, we have that $\mathcal{B} = [0, 1]$ and \mathbf{b} is uniquely determined by $\mathbf{b}(1)$. For ease of notation, we use \mathbf{b} as a

shorthand for $\mathbf{b}(1)$. To show that \mathcal{S} is convex, we need to show that $\mathbf{b}', \mathbf{b}'' \in \mathcal{S} \implies \lambda \mathbf{b}' + (1 - \lambda) \mathbf{b}'' \in \mathcal{S}$ for any $\lambda \in [0, 1]$. Since $J_D^*(\mathbf{b})$ is concave (Lemma 2), we have

$$J_D^*(\lambda \mathbf{b}' + (1 - \lambda) \mathbf{b}'') \geq \lambda J_D^*(\mathbf{b}') + (1 - \lambda) J_D^*(\mathbf{b}'').$$

As $\mathbf{b}', \mathbf{b}'' \in \mathcal{S}$, the optimal action given \mathbf{b}' or \mathbf{b}'' is S . Thus $J_D^*(\mathbf{b}') = Q_D^*(\mathbf{b}', S)$ and $J_D^*(\mathbf{b}'') = Q_D^*(\mathbf{b}'', S)$, where Q_D^* is the optimal Q-function in \mathcal{M}_D^P . Since $Q_D^*(\mathbf{b}, S) = \mathbb{E}_S[c(S, S) \mid \mathbf{b}] = \mathbf{b}c(1, S) + (1 - \mathbf{b})c(0, S)$, we obtain

$$\begin{aligned}
J_D^*(\lambda \mathbf{b}' + (1 - \lambda) \mathbf{b}'') &\geq \lambda J_D^*(\mathbf{b}') + (1 - \lambda) J_D^*(\mathbf{b}'') \\
&= \lambda Q_D^*(\mathbf{b}', S) + (1 - \lambda) Q_D^*(\mathbf{b}'', S) \\
&= \lambda (\mathbf{b}'c(1, S) + (1 - \mathbf{b}')c(0, S)) + \\
&\quad (1 - \lambda) (\mathbf{b}''c(1, S) + (1 - \mathbf{b}'')c(0, S)) \\
&= (\lambda \mathbf{b}' + (1 - \lambda) \mathbf{b}'')c(1, S) \\
&\quad + (\lambda(1 - \mathbf{b}') + (1 - \lambda)(1 - \mathbf{b}''))c(0, S) \\
&= Q_D^*(\lambda \mathbf{b}' + (1 - \lambda) \mathbf{b}'', S) \\
&\geq J_D^*(\lambda \mathbf{b}' + (1 - \lambda) \mathbf{b}'') \quad (J_D^*(\mathbf{b}) = \min_{a^{(D)}} Q_D^*(\mathbf{b}, a^{(D)})) \\
&\implies Q_D^*(\lambda \mathbf{b}' + (1 - \lambda) \mathbf{b}'', S) = J_D^*(\lambda \mathbf{b}' + (1 - \lambda) \mathbf{b}'') \\
&\implies \lambda \mathbf{b}' + (1 - \lambda) \mathbf{b}'' \in \mathcal{S} \quad \forall \lambda \in [0, 1].
\end{aligned}$$

\square

Lemma 4. If $s_t = N$, then $a_t^{(A)} = C$ is a **best response** for any $\mathbf{b}_t \in \mathcal{B}$ and $\pi_D \in \Pi_D$.

Proof. Let J_A^* and Q_A^* be the optimal cost-to-go function and Q-function in \mathcal{M}_A^P . Assume by contradiction that $a_t^{(A)} = C$ is not a **best response**. Then the expected cost of $a_t^{(A)} = S$ must be lower than that of $a_t^{(A)} = C$, i.e.,

$$\begin{aligned}
Q_A^*((\mathbf{b}_t, N), S) &< Q_A^*((\mathbf{b}_t, N), C) \stackrel{(a)}{\implies} \\
\mathbb{E}_{A_t^{(D)}, \mathbf{B}_{t+1}} [-c(s_t, A_t^{(D)}) + \gamma J_A^*(\mathbf{B}_{t+1}) \mid s_t = N, a_t^{(A)} = S] &< \\
\mathbb{E}_{A_t^{(D)}, \mathbf{B}_{t+1}} [-c(s_t, A_t^{(D)}) + \gamma J_A^*(\mathbf{B}_{t+1}) \mid s_t = N, a_t^{(A)} = C] &\stackrel{(b)}{\implies} \\
\mathbb{E}_{A_t^{(D)}, S_{t+1}} \left[\sum_{o \in \mathcal{O}} z(o \mid S_{t+1}) J_A^*(\mathbf{B}(\mathbf{b}_t, A_t^{(D)}, o, \pi_A)) \mid N, S \right] & \\
< \mathbb{E}_{A_t^{(D)}, S_{t+1}} \left[\sum_{o \in \mathcal{O}} z(o \mid S_{t+1}) J_A^*(\mathbf{B}(\mathbf{b}_t, A_t^{(D)}, o, \pi_A)) \mid N, C \right] &
\end{aligned}$$

$\stackrel{(c)}{\implies} 0 < 0$ (contradiction),

where π_A is the attacker strategy assumed by π_D and \mathbb{B} is defined in (6). Step (a) follows from Bellman's optimality equation [101, Eq. 1]; (b) follows because c (7) is independent of $a_t^{(A)}$; and (c) follows because both $a_t^{(A)} = C$ and $a_t^{(A)} = S$ lead to the same state when $s_t = N$ (2). \square

Lemma 5. *If $\pi_D(S | \mathbf{b}_t) = 1$ for some $\mathbf{b}_t \in \mathcal{B}$, then $a_t^{(A)} = C$ is a best response.*

Proof. Assume by contradiction that $a_t^{(A)} = C$ is not a best response. Then the expected cost of $a_t^{(A)} = S$ must be lower than that of $a_t^{(A)} = C$, i.e.,

$$\begin{aligned} Q_A^*((\mathbf{b}_t, s_t), S) &< Q_A^*((\mathbf{b}_t, s_t), C) \stackrel{(a)}{\implies} J_A^*(\mathbf{e}_1) < J_A^*(\mathbf{e}_1) \\ &\stackrel{(b)}{\implies} 0 < 0 \quad (\text{contradiction}), \end{aligned}$$

where (a) follows because c (7) is independent of $a_t^{(A)}$ and because $\pi_D(S | \mathbf{b}_t) = 1 \implies \mathbf{b}_{t+1} = \mathbf{e}_1$ (2). \square

A. Proof of Theorem 1.A

Lemma 3 and the assumption that $N = 1$ means that $\mathcal{S} = [\alpha^*, \kappa]$, where $0 \leq \alpha^* \leq \kappa \leq 1$. Thus, it suffices to show that $\kappa = 1$. Bellman's optimality equation [101, Eq. 1] implies that

$$\begin{aligned} \pi_D^*(\mathbf{e}_2) &\in \arg \min_{a \in \{S, C\}} \left[\overbrace{c(1, S) + \gamma J_D^*(\mathbf{e}_1)}^S, \overbrace{c(1, C) + \gamma J_D^*(\mathbf{e}_2)}^C \right] \\ &\stackrel{(a)}{=} \arg \min_{a \in \{S, C\}} \left[c(1, S) + \gamma J_D^*(\mathbf{e}_1), \right. \\ &\quad \left. \gamma^{\tau-1} c(1, S) + \gamma^\tau J_D^*(\mathbf{e}_1) + \sum_{t=1}^{\tau-1} \gamma^{t-1} c(1, C) \right] \\ &= \arg \min_{a_t^{(D)} \in \{S, C\}} \left[q - r + \gamma J_D^*(\mathbf{e}_1), \right. \\ &\quad \left. \gamma^{\tau-1} (q - r) + \gamma^\tau J_D^*(\mathbf{e}_1) + \left(\frac{1 - \gamma^{\tau-1}}{1 - \gamma} \right) 1^p \right] \stackrel{(b)}{=} \{S\}, \end{aligned}$$

where $\tau \geq 1$ denotes the stopping time; $\mathbf{e}_2 = (0, 1)$; $\mathbf{e}_1 = (1, 0)$; and J_D^* is the optimal cost-to-go function. Step (a) follows because $s = 1$ is an absorbing state until the stop. Step (b) follows from (7) and the fact that $1 > q - r$, which implies that the cost per time-step is upper bounded by $c(N, C) = N^p = 1^p = 1 > q - r$. Thus, $\mathcal{S} = [\alpha^*, 1]$. \square

B. Proof of Theorem 1.B

Since $N = 1$, we have that $\mathcal{B} = [0, 1]$ and \mathbf{b} is uniquely determined by $\mathbf{b}(1)$. For ease of notation, we use \mathbf{b} as a shorthand for $\mathbf{b}(1)$. Given Lemma 4, it suffices to consider the case when $s_t = 0$. From Lemma 5 and the assumption that π_D satisfies (10a), we know that $a_t^{(A)} = S$ is a best response iff $\mathbf{b}_t \in [0, \alpha^*)$, where $\alpha^* \leq 1$. It further follows from Lemma 5 that $\alpha^* = 0 \implies \beta^* = 0$. Thus Thm. 1.B holds when $\alpha^* = 0$. Now consider $\alpha^* > 0$. We know from Lemma 2 and Lemma 3 that the stopping set $\mathcal{S}_A \subset \mathcal{B}$ for the attacker is a convex subset of $[0, \alpha^*)$. Since $0 \in \mathcal{S}_A$ by assumption, it follows that $\mathcal{S}_A = [0, \beta^*]$ for some β^* . \square

APPENDIX B PROOF OF THEOREM 3

As (13) implements one step of the policy iteration algorithm [59, Eqs. 6.4.1-22], (14a) follows from standard results in dynamic programming theory, see e.g., [60, Prop. 1].

To prove (14b), we adapt the proof in [102, Prop 5.1.1]. Let $\tilde{\pi} \triangleq (\pi_{k,t}, \bar{\pi}_{-k,t})$ and $\pi \triangleq (\pi_{k,1}, \bar{\pi}_{-k,t})$. Then define

$$(T_{k,\pi} J_k)(\mathbf{b}_t) \triangleq \mathbb{E}_\pi [c(S_t, A_t^{(D)}) + \gamma J_k(\mathbf{B}_{t+1}) | \pi] \quad \forall \mathbf{b} \in \mathcal{B}.$$

Since $J_k^{(\pi)}$ is a fixed point of $T_{k,\pi}$, i.e., $T_{k,\pi} J_k^{(\pi)} = J_k^{(\pi)}$, and since $T_{k,\pi}^k$ is a contraction mapping [59, Prop. 6.2.4], we have that $\lim_{j \rightarrow \infty} T_{k,\pi}^j J = J_k^{(\pi)}$ for any J [59, Thm. 6.4.6, Cor. 6.4.7]. As a consequence

$$\|\bar{J}_k^{(\tilde{\pi})} - J_k^*\| = \lim_{j \rightarrow \infty} \|T_{k,\tilde{\pi}}^j J_k^* - J_k^*\|. \quad (22)$$

By repeated application of the triangle inequality:

$$\begin{aligned} \|T_{k,\tilde{\pi}}^j J_k^* - J_k^*\| &\leq \|T_{k,\tilde{\pi}}^j J_k^* - T_{k,\tilde{\pi}}^{j-1} J_k^*\| + \|T_{k,\tilde{\pi}}^{j-1} J_k^* - J_k^*\| \\ &\leq \dots \leq \sum_{m=1}^j \|T_{k,\tilde{\pi}}^m J_k^* - T_{k,\tilde{\pi}}^{m-1} J_k^*\|. \end{aligned}$$

Since $T_{k,\tilde{\pi}}$ is a contraction mapping with modulus $\gamma < 1$,

$$\begin{aligned} \|T_{k,\tilde{\pi}}(T_{k,\tilde{\pi}} J_k^*) - T_{k,\tilde{\pi}} J_k^*\| &\leq \gamma \|T_{k,\tilde{\pi}} J_k^* - J_k^*\| \\ \implies \|T_{k,\tilde{\pi}}^j J_k^* - T_{k,\tilde{\pi}}^{j-1} J_k^*\| &\leq \gamma^{j-1} \|T_{k,\tilde{\pi}} J_k^* - J_k^*\|. \end{aligned}$$

The above inequality means that

$$\sum_{m=1}^j \|T_{k,\tilde{\pi}}^m J_k^* - T_{k,\tilde{\pi}}^{m-1} J_k^*\| \leq \sum_{m=1}^j \gamma^{m-1} \|T_{k,\tilde{\pi}} J_k^* - J_k^*\|.$$

Since limits preserve non-strict inequalities,

$$\begin{aligned} \lim_{j \rightarrow \infty} \|T_{k,\tilde{\pi}}^j J_k^* - J_k^*\| &\leq \lim_{j \rightarrow \infty} \sum_{m=1}^j \gamma^{m-1} \|T_{k,\tilde{\pi}} J_k^* - J_k^*\| \\ &= \frac{\|T_{k,\tilde{\pi}} J_k^* - J_k^*\|}{1 - \gamma}. \end{aligned} \quad (23)$$

Now let $\hat{J}_k^{(\tilde{\pi})} \triangleq T_{k,\ell_k}^{\bar{\pi}_{-k,t}} \bar{J}_k^{(\tilde{\pi})}$, where $T_{k,\ell_k}^{\bar{\pi}_{-k,t}}$ is defined in (13). Note that, since Thm. 3 assumes correct conjectures, $T_{k,\tilde{\pi}} \hat{J}_k^{(\tilde{\pi})} = T_{k,1}^{\bar{\pi}_{-k,t}} \hat{J}_k^{(\tilde{\pi})}$ and $T_{k,1}^{\bar{\pi}_{-k,t}} J_k^* = J_k^*$ by definition.

Applying the triangle inequality to the numerator in (23),

$$\begin{aligned} \|T_{k,\tilde{\pi}} J_k^* - J_k^*\| &\leq \|T_{k,\tilde{\pi}} J_k^* - T_{k,\tilde{\pi}} \hat{J}_k^{(\tilde{\pi})}\| + \\ &\|T_{k,\tilde{\pi}} \hat{J}_k^{(\tilde{\pi})} - T_{k,1}^{\bar{\pi}_{-k,t}} \hat{J}_k^{(\tilde{\pi})}\| + \|T_{k,1}^{\bar{\pi}_{-k,t}} \hat{J}_k^{(\tilde{\pi})} - J_k^*\| \\ &= \underbrace{\|T_{k,\tilde{\pi}} J_k^* - T_{k,\tilde{\pi}} \hat{J}_k^{(\tilde{\pi})}\|}_{\leq \gamma \|\hat{J}_k^{(\tilde{\pi})} - J_k^*\|} + \underbrace{\|T_{k,1}^{\bar{\pi}_{-k,t}} \hat{J}_k^{(\tilde{\pi})} - T_{k,1}^{\bar{\pi}_{-k,t}} J_k^*\|}_{\leq \gamma \|\hat{J}_k^{(\tilde{\pi})} - J_k^*\|} \\ &\leq 2\gamma \|\hat{J}_k^{(\tilde{\pi})} - J_k^*\| = 2\gamma \|T_{k,\ell_k}^{\bar{\pi}_{-k,t}} \bar{J}_k^{(\tilde{\pi})} - T_{k,\ell_k}^{\bar{\pi}_{-k,t}} J_k^*\| \\ &\leq 2\gamma^{\ell_k} \|\bar{J}_k^{(\tilde{\pi})} - J_k^*\|. \end{aligned} \quad (24)$$

Combining (22)–(24) gives (14b). \square

APPENDIX C
PROOF OF THEOREM 4.A

The idea behind the proof is to express μ_t (15b) in terms of log-likelihood ratios, which can be shown to converge using the martingale convergence theorem [103, Thm. 6.4.3]. Towards this proof, we prove the following two lemmas.

Lemma 6. Any sequence $(\pi_{\mathbf{h}_t})_{t \geq 1}$ generated by COL induces a well-defined probability measure $\mathbb{P}^{\mathcal{R}}$ over the set of realizable histories $\mathbf{h}_t \in \times_{i=1}^t (\mathcal{H}_i^{(D)} \times \mathcal{H}_i^{(A)})$.

Proof. Since the sample space of the random vectors $(\mathbf{I}_t^{(D)}, \mathbf{I}_t^{(A)})$ (3) is finite (and measurable) for each t , the space of realizable histories $\mathbf{h}_t \in \mathcal{H}_t^{(D)} \times \mathcal{H}_t^{(A)}$ is countable. By the extension theorem of Ionescu Tulcea, it thus follows that a measure $\mathbb{P}^{\mathcal{R}}$ over $\mathcal{H}_t^{(D)} \times \mathcal{H}_t^{(A)}$ exists for all $t \geq 1$ [104]. \square

Lemma 7. For any $\bar{\ell}_A \in \mathcal{L}$ and any sequence $(\nu_t, \pi_{\mathbf{h}_t})_{t \geq 1}$ generated by COL, the following holds a.s.- $\mathbb{P}^{\mathcal{R}}$ as $t \rightarrow \infty$

$$\underbrace{\left| t^{-1} \sum_{\tau=1}^t \ln \frac{\mathbb{P}[\mathbf{i}_{\tau+1}^{(D)} | \ell_A, \mathbf{b}_\tau]}{\mathbb{P}[\mathbf{i}_{\tau+1}^{(D)} | \bar{\ell}_A, \mathbf{b}_\tau]} - K(\bar{\ell}_A, \nu_t) \right|}_{\triangleq Z_{t+1}(\bar{\ell}_A)} = 0.$$

Proof. By definition of Z_t and ν_t ,

$$\begin{aligned} Z_{t+1}(\bar{\ell}_A) &= \sum_{\mathbf{b} \in \mathcal{B}} \sum_{\tau=1}^t t^{-1} \mathbb{1}_{\{\mathbf{b}\}}(\mathbf{b}_\tau) \ln \frac{\mathbb{P}[\mathbf{i}_{\tau+1}^{(D)} | \ell_A, \mathbf{b}_\tau]}{\mathbb{P}[\mathbf{i}_{\tau+1}^{(D)} | \bar{\ell}_A, \mathbf{b}_\tau]} \\ &= \mathbb{E}_{\mathbf{b} \sim \nu_t} \left[\sum_{\tau=1}^t \frac{\ln \mathbb{P}[\mathbf{i}_{\tau+1}^{(D)} | \ell_A, \mathbf{b}]}{t} - \sum_{\tau=1}^t \frac{\ln \mathbb{P}[\mathbf{i}_{\tau+1}^{(D)} | \bar{\ell}_A, \mathbf{b}]}{t} \right], \end{aligned}$$

where we use $\sum_{\mathbf{b} \in \mathcal{B}} \mathbb{1}_{\mathbf{b}_\tau = \mathbf{b}} = 1$. This means that if the left sum above converges to $\mathbb{E}_{\mathbf{I}^{(D)}} [\ln \mathbb{P}[\mathbf{I}^{(D)} | \ell_A, \mathbf{b}]]$ and the right sum converges to $\mathbb{E}_{\mathbf{I}^{(D)}} [\ln \mathbb{P}[\mathbf{I}^{(D)} | \bar{\ell}_A, \mathbf{b}]]$, we obtain $Z_t \xrightarrow{t \rightarrow \infty} K(\bar{\ell}_A, \nu_t)$, which yields the desired result. As these two proofs are almost identical, we only provide the first proof here.

Let $X_\tau \triangleq \ln \mathbb{P}[\mathbf{i}_{\tau+1}^{(D)} | \ell_A, \mathbf{b}_\tau] - \mathbb{E}_{\mathbf{I}^{(D)}} [\ln \mathbb{P}[\mathbf{I}^{(D)} | \ell_A, \mathbf{b}_\tau]]$. We will show that $(X_\tau)_{\tau \geq 1}$ is a martingale difference sequence (MDS). To show this, we need to prove that (i) $\mathbb{E}[X_\tau | \mathbf{h}_{\tau-1}] = 0$; and (ii) $\mathbb{E}[|X_\tau|] < \infty$. We start with (i),

$$\begin{aligned} \mathbb{E}[X_\tau | \mathbf{h}_{\tau-1}] &= \mathbb{E}_{\mathbf{I}^{(D)}} \left[\ln \mathbb{P}[\mathbf{I}^{(D)} | \ell_A, \mathbf{b}_\tau] - \mathbb{E}_{\mathbf{I}^{(D)}} \left[\ln \mathbb{P}[\mathbf{I}^{(D)} | \ell_A, \mathbf{b}_\tau] \right] \middle| \mathbf{h}_{\tau-1} \right] \\ &\stackrel{(a)}{=} \mathbb{E}_{\mathbf{I}^{(D)}} \left[\ln \mathbb{P}[\mathbf{I}^{(D)} | \ell_A, \mathbf{b}_\tau] \right] - \mathbb{E}_{\mathbf{I}^{(D)}} \left[\ln \mathbb{P}[\mathbf{I}^{(D)} | \ell_A, \mathbf{b}_\tau] \right] = 0, \end{aligned}$$

where (a) follows because $\mathbf{I}^{(D)}$ is conditionally independent of $\mathbf{h}_{\tau-1}$ given \mathbf{b}_τ (5).

To prove (ii) we will write X_τ as an expression of the form $(\ln \mathbb{P}[\varphi])^2 \mathbb{P}[\varphi]$, which is bounded by 1³. Towards this end, we start by applying Jensen's inequality to obtain

$$\mathbb{E}[|X_\tau|] = (\mathbb{E}[|X_\tau|^2])^{1/2} \leq (\mathbb{E}[X_\tau^2])^{1/2}, \quad (25)$$

which means that it suffices to bound $\mathbb{E}[X_\tau^2]$.

³We use the standard convention that $(\ln 0)^2 0 = 0$.

Next, we write $\ln \mathbb{P}[\mathbf{i}_{\tau+1}^{(D)} | \ell_A, \mathbf{b}_\tau]$ as

$$\begin{aligned} &\sum_{\mathbf{I}^{(D)}} \mathbb{1}_{\{\mathbf{I}^{(D)}\}}(\mathbf{i}_{\tau+1}^{(D)}) \frac{\mathbb{P}[\mathbf{I}^{(D)} | \ell_A, \mathbf{b}_\tau]}{\mathbb{P}[\mathbf{I}^{(D)} | \ell_A, \mathbf{b}_\tau]} \ln \mathbb{P}[\mathbf{I}^{(D)} | \ell_A, \mathbf{b}_\tau] \\ &= \frac{\mathbb{E}_{\mathbf{I}^{(D)}} \left[\mathbb{1}_{\{\mathbf{I}^{(D)}\}}(\mathbf{i}_{\tau+1}^{(D)}) \ln \mathbb{P}[\mathbf{I}^{(D)} | \ell_A, \mathbf{b}_\tau] \right]}{\mathbb{P}[\mathbf{i}_{\tau+1}^{(D)} | \ell_A, \mathbf{b}_\tau]}, \end{aligned}$$

which means that we can write X_τ as

$$\frac{\mathbb{E}_{\mathbf{I}^{(D)}} \left[\kappa \left(\mathbb{1}_{\{\mathbf{I}^{(D)}\}}(\mathbf{i}_{\tau+1}^{(D)}) - \mathbb{P}[\mathbf{i}_{\tau+1}^{(D)} | \ell_A, \mathbf{b}_\tau] \right) \middle| \ell_A, \mathbf{b}_\tau \right]}{\mathbb{P}[\mathbf{i}_{\tau+1}^{(D)} | \ell_A, \mathbf{b}_\tau]}, \quad (26)$$

where $\kappa \triangleq \ln \mathbb{P}[\mathbf{I}^{(D)} | \ell_A, \mathbf{b}_\tau]$.

Since we focus on realizable histories, we have that $\mathbb{P}[\mathbf{i}_{\tau+1}^{(D)} | \ell_A, \mathbf{b}_\tau] \in (0, 1]$. Hence, it is safe to suppress the denominator in (26). Consequently, the square of (26) can be bounded by the Cauchy-Schwarz inequality as

$$\leq \mathbb{E}_{\mathbf{I}^{(D)}} \left[\kappa^2 \left(\underbrace{\mathbb{1}_{\{\mathbf{I}^{(D)}\}}(\mathbf{i}_\tau^{(D)} + 1) - \mathbb{P}[\mathbf{i}_{\tau+1}^{(D)} | \ell_A, \mathbf{b}_\tau]}_{\triangleq \chi} \right)^2 \middle| \ell_A, \mathbf{b}_\tau \right].$$

Next, since $\kappa \geq 0$ and $\chi \in [0, 1]$, we obtain that

$$X_\tau^2 \leq \mathbb{E}_{\mathbf{I}^{(D)}} \left[\kappa^2 \chi^2 \middle| \ell_A, \mathbf{b}_\tau \right] \leq \mathbb{E}_{\mathbf{I}^{(D)}} \left[\kappa^2 \middle| \ell_A, \mathbf{b}_\tau \right],$$

which means that

$$\begin{aligned} \mathbb{E}[X_\tau^2] &\leq \mathbb{E}_{\mathbf{I}^{(D)}} \left[\mathbb{P}[\mathbf{I}^{(D)} | \ell_A, \mathbf{b}_\tau] \ln^2 \mathbb{P}[\mathbf{I}^{(D)} | \ell_A, \mathbf{b}_\tau] \middle| \ell_A, \mathbf{b}_\tau \right] \leq 1 \\ &\stackrel{(a)}{\implies} \mathbb{E}[|X_\tau|] \leq 1, \end{aligned}$$

where (a) follows from (25). Therefore, $(X_\tau)_{\tau \geq 1}$ is an MDS. Consequently, the sequence $Y_t \triangleq \sum_{\tau=1}^t \frac{X_\tau}{\tau}$ is a martingale. By the martingale convergence theorem, $(Y_\tau)_{\tau \geq 1}$ converges to a finite and integrable random variable a.s.- $\mathbb{P}^{\mathcal{R}}$ [103, Thm. 6.4.3]. This convergence means that we can invoke Kronecker's lemma, which states that $\lim_{t \rightarrow \infty} t^{-1} \sum_{\tau=1}^t X_\tau = 0$ a.s.- $\mathbb{P}^{\mathcal{R}}$ [105, pp. 105]. As a consequence, the following holds a.s.- $\mathbb{P}^{\mathcal{R}}$ as $t \rightarrow \infty$

$$\mathbb{E}_{\mathbf{b} \sim \nu_t} \sum_{\tau=1}^t \frac{\ln \mathbb{P}[\mathbf{i}_{\tau+1}^{(D)} | \ell_A, \mathbf{b}]}{t} = \mathbb{E}_{\mathbf{b} \sim \nu_t} \mathbb{E}_{\mathbf{I}^{(D)}} \left[\ln \mathbb{P}[\mathbf{I}^{(D)} | \ell_A, \mathbf{b}] \right].$$

\square

A. Proof of Theorem 4.A

To streamline analysis, we treat μ_t as a probability measure over \mathcal{L} and use integral language. From Bayes rule and the Markov property of $\mathbb{P}[\mathbf{I}^{(D)} | \bar{\ell}_A, \mathbf{b}_t]$, we have that

$$\begin{aligned} \mu_{t+1}(\bar{\ell}_A) &= \frac{\mathbb{P}[\bar{\ell}_A] \mathbb{P}[\mathbf{i}_2^{(D)}, \dots, \mathbf{i}_{t+1}^{(D)} | \bar{\ell}_A, \mathbf{h}_t^{(D)}]}{\mathbb{P}[\mathbf{i}_2^{(D)}, \dots, \mathbf{i}_{t+1}^{(D)} | \mathbf{h}_t^{(D)}]} \\ &\stackrel{(a)}{=} \frac{\mu_1(\bar{\ell}_A) \prod_{\tau=1}^t \mathbb{P}[\mathbf{i}_{\tau+1}^{(D)} | \bar{\ell}_A, \mathbf{b}_\tau]}{\int_{\mathcal{L}} \mu_1(d\bar{\ell}_A) \prod_{\tau=1}^t \mathbb{P}[\mathbf{i}_{\tau+1}^{(D)} | \bar{\ell}_A, \mathbf{b}_\tau]} \\ &= \frac{\mu_1(\bar{\ell}_A) \exp \left(\ln \left(\prod_{\tau=1}^t \frac{\mathbb{P}[\mathbf{i}_{\tau+1}^{(D)} | \bar{\ell}_A, \mathbf{b}_\tau]}{\mathbb{P}[\mathbf{i}_{\tau+1}^{(D)} | \ell_A, \mathbf{b}_\tau]} \right) \right)}{\int_{\mathcal{L}} \mu_1(d\bar{\ell}_A) \exp \left(\ln \left(\prod_{\tau=1}^t \frac{\mathbb{P}[\mathbf{i}_{\tau+1}^{(D)} | \bar{\ell}_A, \mathbf{b}_\tau]}{\mathbb{P}[\mathbf{i}_{\tau+1}^{(D)} | \ell_A, \mathbf{b}_\tau]} \right) \right)} \end{aligned}$$

$$= \frac{\mu_1(\bar{\ell}_A) \exp(-tZ_{t+1}(\bar{\ell}_A))}{\int_{\mathcal{L}} \mu_1(d\bar{\ell}_A) \exp(-tZ_{t+1}(\bar{\ell}_A))}, \quad (27)$$

where Z_t is defined in Lemma 7. Step (a) above is well-defined by Assumption 1 and follows because $\mathbf{I}^{(D)}$ is conditionally independent of $\mathbf{h}_{t-1}^{(D)}$ given \mathbf{b}_{t-1} .

Using the expression in (27), we obtain that

$$\begin{aligned} & \mathbb{E}_{\bar{\ell}_A \sim \mu_{t+1}} \left[\overbrace{K(\bar{\ell}_A, \nu_t) - K_{\mathcal{L}}^*(\nu_t)}^{\triangleq \Delta K(\bar{\ell}_A, \nu_t)} \right] \\ &= \frac{\int_{\mathcal{L}} \Delta K(\bar{\ell}_A, \nu_t) \mu_1(d\bar{\ell}_A) \exp(-tZ_{t+1}(\bar{\ell}_A))}{\int_{\mathcal{L}} \mu_1(d\bar{\ell}_A) \exp(-tZ_{t+1}(\bar{\ell}_A))} \\ &= \frac{\int_{\mathcal{L}} \overbrace{\Delta K(\bar{\ell}_A, \nu_t) \mu_1(d\bar{\ell}_A) \exp(-t(Z_{t+1}(\bar{\ell}_A) - K_{\mathcal{L}}^*(\nu_{t+1})))}^{\triangleq \sigma}}{\int_{\mathcal{L}} \mu_1(d\bar{\ell}_A) \exp(-t(Z_{t+1}(\bar{\ell}_A) - K_{\mathcal{L}}^*(\nu_{t+1})))}. \end{aligned} \quad (28)$$

By defining $\mathcal{L}_\epsilon \triangleq \{\bar{\ell}_A \mid \Delta K(\bar{\ell}_A, \nu_{t+1}) \geq \epsilon\}$, we can write the numerator in (28) as

$$\int_{\mathcal{L} \setminus \mathcal{L}_\epsilon} \sigma + \int_{\mathcal{L}_\epsilon} \sigma \leq \epsilon + \int_{\mathcal{L} \setminus \mathcal{L}_\epsilon} \sigma. \quad (29)$$

Given this bound, it suffices to show that

$$\lim_{t \rightarrow \infty} \frac{\int_{\mathcal{L}_\epsilon} \sigma}{\int_{\mathcal{L}} \mu_1(d\bar{\ell}_A) \exp(-t(Z_{t+1}(\bar{\ell}_A) - K_{\mathcal{L}}^*(\nu_{t+1})))} = 0,$$

for arbitrarily small $\epsilon > 0$. Towards this proof, we note that the exponent in σ (28) can be written as

$$\begin{aligned} & -t(Z_{t+1}(\bar{\ell}_A) - K_{\mathcal{L}}^*(\nu_{t+1})) \\ &= -t(Z_{t+1}(\bar{\ell}_A) - K_{\mathcal{L}}^*(\nu_{t+1})) + K(\bar{\ell}_A, \nu_{t+1}) - K(\bar{\ell}_A, \nu_{t+1}) \\ &= -t(\Delta K(\bar{\ell}_A, \nu_{t+1}) + Z_{t+1}(\bar{\ell}_A) - K(\bar{\ell}_A, \nu_{t+1})). \end{aligned} \quad (30)$$

Next, we recall from Lemma 7 that for any $\epsilon > 0$, there exists $\eta > 0$ and $t_\eta \geq 1$ such that, for all $t \geq t_\eta$ and $\bar{\ell}_A \in \mathcal{L}$, $|Z_t(\bar{\ell}_A - K(\bar{\ell}_A, \nu_{t+1}))| < \eta$. (t_η is uniform as $|\mathcal{L}| < \infty$, Assumption 1.) This fact together with (30) implies that

$$\begin{aligned} & \frac{\int_{\mathcal{L}_\epsilon} \Delta K(\bar{\ell}_A, \nu_{t+1}) \mu_1(d\bar{\ell}_A) \exp(-t(Z_{t+1}(\bar{\ell}_A) - K_{\mathcal{L}}^*(\nu_{t+1})))}{\int_{\mathcal{L}} \mu_1(d\bar{\ell}_A) \exp(-t(Z_{t+1}(\bar{\ell}_A) - K_{\mathcal{L}}^*(\nu_{t+1})))} \\ & \leq \frac{\int_{\mathcal{L}_\epsilon} \Delta K(\bar{\ell}_A, \nu_{t+1}) \mu_1(d\bar{\ell}_A) \exp(-t(\Delta K(\bar{\ell}_A, \nu_{t+1}) - \eta))}{\int_{\mathcal{L}} \mu_1(d\bar{\ell}_A) \exp(-t(\Delta K(\bar{\ell}_A, \nu_{t+1}) + \eta))} \\ & = e^{2t\eta} \frac{\int_{\mathcal{L}_\epsilon} \Delta K(\bar{\ell}_A, \nu_{t+1}) \mu_1(d\bar{\ell}_A) e^{-t\Delta K(\bar{\ell}_A, \nu_{t+1})}}{\int_{\mathcal{L}} \mu_1(d\bar{\ell}_A) e^{-t\Delta K(\bar{\ell}_A, \nu_{t+1})}} \quad (*) \end{aligned}$$

for all $t \geq t_\eta$.

Now, consider the numerator in (*). Since xe^{-tx} is decreasing for all $x > t^{-1}$ and since $\Delta K(\bar{\ell}_A, \nu_{t+1}) \geq \epsilon$ for all $\bar{\ell}_A \in \mathcal{L}_\epsilon$, we have that

$$\int_{\mathcal{L}_\epsilon} \Delta K(\bar{\ell}_A, \nu_{t+1}) \mu_1(d\bar{\ell}_A) e^{-t\Delta K(\bar{\ell}_A, \nu_{t+1})} \leq \epsilon e^{-t\epsilon}$$

for any $t \geq \max[t_\eta, \frac{1}{\epsilon}]$.

Next, consider the denominator in (*). By definition, $\exists \bar{\ell}_A \in \mathcal{L}$ such that $K(\bar{\ell}_A, \nu_t) = K_{\mathcal{L}}^*(\nu_t) \forall t$. This fact, together with the assumption that μ_1 has full support (Assumption 1), means that the denominator is a positive constant, which we denote by k . As a result, (*) $\leq e^{2t\eta} \epsilon e^{-t\epsilon} k^{-1}$. Let $\eta = \frac{\epsilon}{4}$. Then

$e^{2t\eta} \epsilon e^{-t\epsilon} k^{-1} = e^{\frac{-t\epsilon}{2}} \epsilon k^{-1}$, which converges to 0 as $t \rightarrow \infty$. Consequently, $\lim_{t \rightarrow \infty} \mathbb{E}_{\bar{\ell}_A \sim \mu_t} [\Delta K(\bar{\ell}_A, \nu_t)] = 0$ a.s.- $\mathbb{P}^{\mathcal{B}}$.

APPENDIX D PROOF OF THEOREM 4.B

The proof of Thm. 4.B follows the same procedure as that of Thm. 4.A, with the difference that Θ_k is allowed to be non-finite, whereas \mathcal{L} in Thm. 4.A is finite (Assumption 1).

Define $\Theta_{k,\epsilon}^+ \triangleq \{\bar{\theta} \mid \Delta K(\bar{\theta}, \nu_t) \geq \epsilon\}$ and $\Theta_{k,\frac{\epsilon}{2}}^- \triangleq \{\bar{\theta} \mid \Delta K(\bar{\theta}, \nu_t) \leq \frac{\epsilon}{2}\}$. It then follows from (29) that

$$\begin{aligned} & \int_{\Theta_k} \left(\overbrace{K(\bar{\theta}, \nu_t) - K_{\Theta_k}^*(\nu_t)}^{\Delta K(\bar{\theta}, \nu_t)} \right) \rho_{t+1}^{(k)}(d\bar{\theta}) \leq \epsilon + \\ & \frac{\int_{\Theta_{k,\epsilon}^+} \Delta K(\bar{\theta}, \nu_t) \exp(-t(Z_t(\bar{\theta}) - K_{\Theta_k}^*(\nu_t))) \rho_1^{(k)}(d\bar{\theta})}{\underbrace{\int_{\Theta_{k,\frac{\epsilon}{2}}^-} \exp(-t(Z_t(\bar{\theta}) - K_{\Theta_k}^*(\nu_t))) \rho_1^{(k)}(d\bar{\theta})}_{\triangleq \star}}, \end{aligned} \quad (31)$$

where \star is well-defined by Assumptions 1–2.

(31) implies that it suffices to prove that $\star \xrightarrow{t \rightarrow \infty} 0$ for arbitrarily small ϵ . Applying Lemma 7 and (*), we obtain

$$\begin{aligned} \star & \stackrel{(a)}{\leq} e^{2t\eta} \frac{\int_{\Theta_{k,\epsilon}^+} \Delta K(\bar{\theta}, \nu_t) e^{-t\Delta K(\bar{\theta}, \nu_t)} \rho_1^{(k)}(d\bar{\theta})}{\int_{\Theta_{k,\frac{\epsilon}{2}}^-} e^{-t\Delta K(\bar{\theta}, \nu_t)} \rho_1^{(k)}(d\bar{\theta})} \\ & \stackrel{(b)}{\leq} e^{2t\eta} \frac{\epsilon e^{-t\epsilon}}{\int_{\Theta_{k,\frac{\epsilon}{2}}^-} e^{-t\Delta K(\bar{\theta}, \nu_t)} \rho_1^{(k)}(d\bar{\theta})} \\ & \stackrel{(c)}{\leq} e^{2t\eta} \frac{\epsilon e^{-t\epsilon}}{e^{-t\frac{\epsilon}{2}} \int_{\Theta_{k,\frac{\epsilon}{2}}^-} \rho_1^{(k)}(d\bar{\theta})} = e^{2t\eta} \frac{\epsilon e^{-t\frac{\epsilon}{2}}}{\rho_1^{(k)}(\Theta_{k,\frac{\epsilon}{2}}^-)} \quad (32) \end{aligned}$$

for all $t \geq \max[t_\eta, \epsilon^{-1}]$, where (a) follows from (*); (b) follows because xe^{-tx} is decreasing for all $x > t^{-1}$; and (c) follows because $e^{-t\Delta K(\bar{\theta}, \nu_t)} \geq e^{-t\frac{\epsilon}{2}}$.

Let $\eta = \epsilon/8$. Then the numerator in the final expression above becomes $\epsilon e^{-t\frac{\epsilon}{4}}$, which converges to 0 as $t \rightarrow \infty$. Thus, what remains to show is that the denominator is positive in the limit, i.e., $\lim_{t \rightarrow \infty} \rho_1^{(k)}(\Theta_{k,\frac{\epsilon}{2}}^-) > 0$. We prove this statement by establishing uniform continuity of $\Delta K(\bar{\theta}, \nu)$. Towards this end, we prove the following two lemmas.

Lemma 8. \mathcal{B} (5) is a compact subset of $\mathbb{R}^{|\mathcal{S}|}$ with the Euclidean metric d and $\Delta(\mathcal{B})$ a compact metric space with the Wasserstein- p distance W_p ($p \geq 1$).

Proof. Since \mathcal{S} is finite, $\mathcal{B} = \Delta(\mathcal{S})$ is a compact subset of $\mathbb{R}^{|\mathcal{S}|}$ and (\mathcal{B}, d) is a Polish space. To prove that $(\Delta(\mathcal{B}), W_p)$ is compact we will show that every sequence $(\nu_n)_{n=1}^\infty \subset \Delta(\mathcal{B})$ admits a subsequence converging to some limit point in $\Delta(\mathcal{B})$. Since \mathcal{B} is compact and $\nu_n(\mathcal{B}) = 1$, this collection of measures is tight as $\exists \mathcal{C} \subseteq \mathcal{B}$ such that $\nu_n(\mathcal{C}) = 1 > 1 - \epsilon$ for any $\epsilon > 0$ and ν_n . Therefore, $(\nu_n)_{n=1}^\infty$ admits a limit point $\nu^* \in \Delta(\mathcal{B})$ w.r.t the topology of weak convergence (Prokhorov's theorem [106, Ch. 1, §5]). We will show that ν^* is also a limit point under W_p . By Skorokhod's representation theorem [106, p. 70], there exists a sequence of \mathcal{B} -valued random variables $\{V_1, \dots, V_n, \dots, V^*\}$ such that V_n has the probability law

ν_n and V_n converges to V^* almost surely as $n \rightarrow \infty$. By the dominance convergence theorem and the facts that \mathcal{B} is compact and d is continuous, $\lim_{n \rightarrow \infty} \mathbb{E}[d(V_n, V^*)^p] = 0$. Consequently, for any coupling ξ between ν_n and ν^* ,

$$\lim_{n \rightarrow \infty} \left(\int d(x, y)^p d\xi(x, y) \right)^{\frac{1}{p}} = 0.$$

Since $W_p(\nu_n, \nu^*)$ is the infimum of the left-hand side above (by definition), $\lim_{n \rightarrow \infty} W_p(\nu_n, \nu^*) = 0$. Hence, every sequence $(\nu_n)_{n=1}^\infty \subset \Delta(\mathcal{B})$ admits a subsequence converging to some limit point in $\Delta(\mathcal{B})$ under W_p . Thus, $(\Delta(\mathcal{B}), W_p)$ is compact. \square

Lemma 9. $\Delta K(\bar{\theta}, \nu) \triangleq K(\bar{\theta}, \nu) - K_{\Theta_k}^*(\nu)$ is a continuous map from $(\Theta_k, d) \times (\Delta(\mathcal{B}), W_1)$ to \mathbb{R} , where d and W_1 denote the Euclidean and the Wasserstein-1 distance, respectively.

Proof. We start by showing that $K(\bar{\theta}, \nu)$ is continuous by proving that for any convergent sequence $(\bar{\theta}_n, \nu_n) \xrightarrow{n \rightarrow \infty} (\bar{\theta}, \nu)$, the difference $|K(\bar{\theta}_n, \nu_n) - K(\bar{\theta}, \nu)|$ converges to 0. This difference can be bounded by the triangle inequality as

$$\begin{aligned} |K(\bar{\theta}_n, \nu_n) - K(\bar{\theta}, \nu)| &\leq \\ &\underbrace{|K(\bar{\theta}_n, \nu_n) - K(\bar{\theta}_n, \nu)|}_{\triangleq \textcircled{1}} + \underbrace{|K(\bar{\theta}_n, \nu) - K(\bar{\theta}, \nu)|}_{\triangleq \textcircled{2}}. \end{aligned}$$

Consider the left expression above (①). (16) implies that

$$\begin{aligned} \textcircled{1} &= \left| \int_{\mathcal{B}} \mathbb{E}_{\mathbf{I}^{(k)}} \left[\ln \left(\frac{\mathbb{P}[\mathbf{I}^{(k)} | \boldsymbol{\theta}, \mathbf{b}]}{\mathbb{P}[\mathbf{I}^{(k)} | \bar{\boldsymbol{\theta}}_n, \mathbf{b}]} \right) \right] \nu_n(d\mathbf{b}) \right. \\ &\quad \left. - \int_{\mathcal{B}} \mathbb{E}_{\mathbf{I}^{(k)}} \left[\ln \left(\frac{\mathbb{P}[\mathbf{I}^{(k)} | \boldsymbol{\theta}, \mathbf{b}]}{\mathbb{P}[\mathbf{I}^{(k)} | \bar{\boldsymbol{\theta}}_n, \mathbf{b}]} \right) \right] \nu(d\mathbf{b}) \right|, \end{aligned}$$

which is an integral probability metric (IPM) with the testing function $f(\mathbf{b}) \triangleq \mathbb{E}_{\mathbf{I}^{(k)}} \left[\ln \left(\frac{\mathbb{P}[\mathbf{I}^{(k)} | \boldsymbol{\theta}, \mathbf{b}]}{\mathbb{P}[\mathbf{I}^{(k)} | \bar{\boldsymbol{\theta}}_n, \mathbf{b}]} \right) \right]$. This function is assumed to be Lipschitz continuous (Assumption 2.1). As the function can be rescaled, we can, without loss of generality, assume the Lipschitz constant to be 1. Since the Wasserstein distance is equivalent to the IPM w.r.t the class of 1-Lipschitz functions, ① is upper-bounded by $W_p(\nu_n, \nu)$. Hence, as ν_n converges to ν in W_p , ① converges to 0. Therefore, $\nu \mapsto K(\bar{\theta}, \nu)$ is continuous. We now show that ② converges. Using Assumption 2.2 and the dominated convergence theorem, we obtain that

$$\begin{aligned} &\lim_{n \rightarrow \infty} \mathbb{E}_{\mathbf{b} \sim \nu} \mathbb{E}_{\mathbf{I}^{(k)}} \left[\ln \left(\frac{\mathbb{P}[\mathbf{I}^{(k)} | \boldsymbol{\theta}, \mathbf{b}]}{\mathbb{P}[\mathbf{I}^{(k)} | \bar{\boldsymbol{\theta}}_n, \mathbf{b}]} \right) \right] \\ &= \mathbb{E}_{\mathbf{b} \sim \nu} \mathbb{E}_{\mathbf{I}^{(k)}} \left[\ln \left(\frac{\mathbb{P}[\mathbf{I}^{(k)} | \boldsymbol{\theta}, \mathbf{b}]}{\mathbb{P}[\mathbf{I}^{(k)} | \bar{\boldsymbol{\theta}}, \mathbf{b}]} \right) \right], \end{aligned}$$

which implies that ② converges to 0 as $n \rightarrow \infty$. Consequently, $\bar{\boldsymbol{\theta}} \mapsto K(\bar{\boldsymbol{\theta}}, \nu)$ is continuous. Finally, since Θ_k is compact (Assumption 1) and $K(\bar{\boldsymbol{\theta}}, \nu)$ is continuous in both $\bar{\boldsymbol{\theta}}$ and ν , we can apply Berge's maximum theorem to $K(\bar{\boldsymbol{\theta}}, \nu)$ w.r.t. $\bar{\boldsymbol{\theta}}$. This theorem states that the mapping $\nu \mapsto K_{\Theta_k}^*(\nu)$ is continuous (17a). Since continuity is preserved under subtraction, it follows that ΔK is also continuous [107, Thm. 17.31]. \square

A. Proof of Theorem 4.B

Lemmas 8–9 and the compactness of Θ_k (Assumption 1) imply uniform continuity of $\Delta K(\bar{\boldsymbol{\theta}}, \nu)$ and that $|\Theta_k^*(\nu)| > 0$ [107, Thm. 17.31]. As a consequence, for each $\bar{\boldsymbol{\theta}}_\nu \in \Theta_k^*(\nu)$, $\bar{\boldsymbol{\theta}}' \in \Theta_k$, and $\nu', \nu \in \Delta(\mathcal{B})$, $\exists \delta_m$ such that $d(\bar{\boldsymbol{\theta}}_\nu, \bar{\boldsymbol{\theta}}') < \delta_m$, $W_1(\nu, \nu') < \delta_m$, and $d(\Delta K(\bar{\boldsymbol{\theta}}', \nu'), \Delta K(\bar{\boldsymbol{\theta}}_\nu, \nu)) \leq m \xrightarrow{(a)} \Delta K(\bar{\boldsymbol{\theta}}', \nu') < m$ for each $m > 0$, where (a) follows because $\bar{\boldsymbol{\theta}}_\nu \in \Theta_k^*(\nu) \implies \Delta K(\bar{\boldsymbol{\theta}}_\nu, \nu) = 0$. Define the ball $B(\nu, \delta_m) \triangleq \{\nu' \mid W_1(\nu, \nu') < \delta_m, \nu' \in \Delta(\mathcal{B})\}$. It follows that, for any $\nu \in \Delta(\mathcal{B})$ and $\nu' \in B(\nu, \delta_m)$,

$$\underbrace{\{\bar{\boldsymbol{\theta}}' \mid d(\bar{\boldsymbol{\theta}}', \bar{\boldsymbol{\theta}}_\nu) < \delta_m\}}_{\Theta_\nu(\delta_m)} \subset \underbrace{\{\bar{\boldsymbol{\theta}}' \mid \Delta K(\bar{\boldsymbol{\theta}}', \nu') \leq m\}}_{\Theta_{\nu'}(m)}.$$

Thus, for any ν and $\nu' \in B(\nu, \delta_m)$,

$$\rho_1^{(k)}(\Theta_{\nu'}(m)) \geq \rho_1^{(k)}(\Theta_\nu(\delta_m)) \stackrel{(a)}{\geq} 0,$$

where (a) follows because $\rho_1^{(k)}$ has full support (Assumption 1).

Since $\Delta(\mathcal{B})$ is compact (Lemma 8), the set $\{B(\nu, \delta_m)\}_{\nu \in \Delta(\mathcal{B})}$ forms an open cover for a compact space, which means that there exists a finite subcover $\{B(\nu_i, \delta_m)\}_{i=1}^M$. As a consequence, each $\nu' \in \Delta(\mathcal{B})$ belongs to some Wasserstein ball $B(\nu_i, \delta_m)$. Let $r \triangleq \min_i \rho_1^{(k)}(\Theta_{\nu_i}(\delta_m)) > 0$. We then have that

$$\rho_1^{(k)}(\Theta_{\nu'}(m)) \geq \rho_1^{(k)}(\Theta_{\nu_i}(\delta_m)) \geq r.$$

Now recall the denominator $\rho_1^{(k)}(\Theta_{k, \frac{\epsilon}{2}}^-)$ in (32). Let $m = \frac{\epsilon}{2}$. Then $\rho_1^{(k)}(\Theta_{k, \frac{\epsilon}{2}}^-) \geq r > 0$ for any $\epsilon > 0$. Hence, $\lim_{t \rightarrow \infty} \frac{\epsilon e^{-t \frac{\epsilon}{4}}}{\rho_1^{(k)}(\Theta_{k, \frac{\epsilon}{2}}^-)} = 0$. \square

APPENDIX E

EXAMPLE DERIVATION OF A BERK-NASH EQUILIBRIUM

We use the following example to illustrate the steps required to find a Berk-Nash equilibrium.

Example 1. Consider Prob. 1 with $N = 1$, $p_A = 1$, $\mathcal{O} = \{0, 1\}$, $z_{\theta_i}(\cdot | 0) = \text{Ber}(p)$, $z_{\theta_i}(1 | 1) = \text{Ber}(q)$, $\mathbf{b}_1(1) = 0$, and c being defined as in Fig. 4. Let the rollout parameters be $(\ell_A = 0, \ell_D = 1)$ and let π_1 be threshold strategies with $\beta \geq 0$ and $\alpha \leq 1$ (Thm. 1). Finally, let $\mathcal{L} = \{\ell_A\}$, $\Theta_A = \{\theta_1\}$, and $\Theta_D = \{\bar{\theta}_a, \bar{\theta}_b\}$, where $z_{\bar{\theta}_a}(0 | 0) = z_{\bar{\theta}_a}(1 | 1) = z_{\bar{\theta}_b}(1 | 0) = z_{\bar{\theta}_b}(0 | 1) = 1$.

First note that the definition of $z_{\bar{\theta}_a}$, $z_{\bar{\theta}_b}$, and \mathbf{b}_1 imply that $\mathbf{b}_t(1) \in \{0, 1\}$ for all t , which simplifies the following derivation. For ease of notation, we write \mathbf{b} instead of $\mathbf{b}(1)$. To derive a BNE, we start with condition (i) in Def. 2. Since $\ell_A = 0$, it suffices to consider π_D . By the principle of optimality

$$\pi_D(\mathbf{b}) \in \arg \min_{a \in A_D} \mathbb{E}_{S, \mathbf{B}'} \left[c(S, a) + \gamma \bar{J}_{D, \bar{\boldsymbol{\theta}}}^{(\pi_1)}(\mathbf{B}') \mid \mathbf{b}, \pi_1 \right].$$

Let $\mathbf{P}_{\bar{\boldsymbol{\theta}}, \pi_1}$ and \mathbf{c}_{π_1} be the belief transition matrix and the vector of expected stage costs induced by $(\bar{\boldsymbol{\theta}}, \pi_1)$, respectively. From the definition of Θ_D we obtain that

$$\mathbf{P}_{\bar{\theta}_a, \pi_1} \stackrel{(a)}{=} \begin{bmatrix} 1 - q & q \\ 1 & 0 \end{bmatrix}, \mathbf{P}_{\bar{\theta}_b, \pi_1} \stackrel{(b)}{=} \begin{bmatrix} 1 - p & p \\ 1 & 0 \end{bmatrix}, \mathbf{c}_{\pi_1} \stackrel{(c)}{=} \begin{bmatrix} 0 \\ -1 \end{bmatrix},$$

where (a)–(c) follow because $\alpha \in (0, 1] \implies \pi_D(1) = S, \pi_D(0) = C$.

By definition, $\bar{J}_{D, \bar{\theta}}^{(\pi_1)} = (\mathbf{1}_2 - \gamma \mathbf{P}_{\bar{\theta}, \pi_1})^{-1} \mathbf{c}_{\pi_1}$, where $\mathbf{1}_2$ is the 2×2 identity matrix. Therefore,

$$\begin{aligned} \bar{J}_{D, \bar{\theta}_a}^{(\pi_1)} &= (\mathbf{1}_2 - \gamma \mathbf{P}_{\bar{\theta}_a, \pi_1})^{-1} \mathbf{c}_{\pi_1} \\ &= \left(\mathbf{1}_2 - \gamma \begin{bmatrix} 1-q & q \\ 1 & 0 \end{bmatrix} \right)^{-1} \begin{bmatrix} 0 \\ -1 \end{bmatrix} \\ &= \begin{bmatrix} 1 - \gamma + \gamma q & -\gamma q \\ -\gamma & 1 \end{bmatrix}^{-1} \begin{bmatrix} 0 \\ -1 \end{bmatrix} \\ &= \begin{bmatrix} \frac{-1}{(\gamma-1)(1+\gamma q)} & \frac{-\gamma q}{(\gamma-1)(1+\gamma q)} \\ \frac{-\gamma}{(\gamma-1)(1+\gamma q)} & \frac{\gamma-1-\gamma q}{(\gamma-1)(1+\gamma q)} \end{bmatrix} \begin{bmatrix} 0 \\ -1 \end{bmatrix} \\ &= \frac{1}{(\gamma-1)(1+\gamma q)} \begin{bmatrix} \gamma q \\ 1 + \gamma(q-1) \end{bmatrix}. \end{aligned}$$

Similarly,

$$\begin{aligned} \bar{J}_{D, \bar{\theta}_b}^{(\pi_1)} &= (\mathbf{1}_2 - \gamma \mathbf{P}_{\bar{\theta}_b, \pi_1})^{-1} \mathbf{c}_{\pi_1} \\ &= \left(\mathbf{1}_2 - \gamma \begin{bmatrix} 1-p & p \\ 1 & 0 \end{bmatrix} \right)^{-1} \begin{bmatrix} 0 \\ -1 \end{bmatrix} \\ &= \frac{1}{(\gamma-1)(1+\gamma p)} \begin{bmatrix} \gamma p \\ 1 + \gamma(p-1) \end{bmatrix}. \end{aligned}$$

Hence, to meet condition (i), the defender's rollout strategy must satisfy $\pi_D(0) = C$ and $\pi_D(1) = S$, which is ensured by (13). As a consequence, $\pi = \pi_1$ in any BNE.

Now consider condition (ii); (16) can be written as

$$\begin{aligned} K(\bar{\theta}, \nu) &= \mathbb{E}_{\mathbf{b} \sim \nu} \mathbb{E}_{\mathbf{I}^{(D)}} \left[\ln \left(\frac{\mathbb{P}[\mathbf{I}^{(D)} \mid \theta, \mathbf{b}]}{\mathbb{P}[\mathbf{I}^{(D)} \mid \bar{\theta}, \mathbf{b}]} \right) \mid \theta, \mathbf{b} \right] \\ &= - \sum_{\mathbf{b} \in \{0,1\}} \nu(\mathbf{b}) \sum_{o \in \{0,1\}} z_{\theta}(o \mid \mathbf{b}) \ln z_{\bar{\theta}}(o \mid \mathbf{b}) + \text{const.} \end{aligned}$$

Minimizing the above expression with respect to $\bar{\theta}$ yields $\Theta_D^* = \{\bar{\theta}_a\}$ if $(p = 0, q = 1)$. Conversely, $\Theta_D^* = \{\bar{\theta}_b\}$ if $(p = 1, q = 0)$. Otherwise, $\Theta_D^*(\nu) = \{\bar{\theta}_a, \bar{\theta}_b\}$.

Lastly, condition (iii) is satisfied iff $\mathbf{P}_{\bar{\theta}, \pi_1}^T \nu = \nu$. Since $\mathbf{P}_{\bar{\theta}, \pi_1}^T = \rho^{(D)}(\bar{\theta}_a) \mathbf{P}_{\bar{\theta}_a, \pi_1}^T + (1 - \rho^{(D)}(\bar{\theta}_a)) \mathbf{P}_{\bar{\theta}_b, \pi_1}^T$, solving this equation gives

$$\nu(0) = - \left(-1 - p + \rho^{(D)}(\bar{\theta}_a) p - \rho^{(D)}(\bar{\theta}_a) q \right)^{-1}, \quad (33)$$

which means the BNE is not unique and may not exist; see Fig. 17 on the next page. For example, if $p = 1$ and $q = 0$, then (33) requires that $\rho^{(D)}(\bar{\theta}_a) = 1$, but this means that $\rho^{(D)} \notin \Delta(\Theta^*(\nu))$, which violates condition (ii).

APPENDIX F HYPERPARAMETERS

The hyperparameters used for the evaluation in this paper are listed in Table 5 and were obtained through grid search.

APPENDIX G CONFIGURATION OF THE INFRASTRUCTURE IN FIG. 1

The configuration of the target infrastructure (Fig. 1) is available in Table 6.

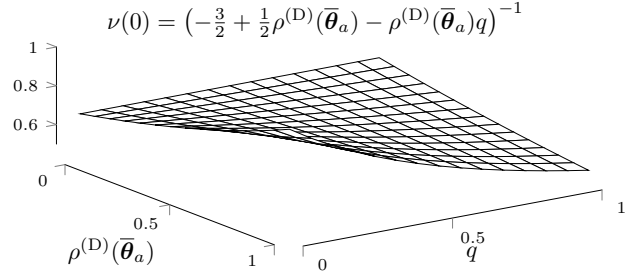


Fig. 17: Berk-Nash equilibria of Ex. 1 when $p = \frac{1}{2}$.

Figures and Tables	Values
Fig. 7	$\mathcal{O} = \{0, \dots, 9\}, p_A = 0.1, \gamma = 0.99$
	$z(\cdot 0) = \text{BetaBin}(n = 10, \alpha = 0.7, \beta = 3)$
	$z(\cdot 1) = \text{BetaBin}(n = 10, \alpha = 1, \beta = 0.7)$
Fig. 6	$\mathcal{O} = \{0, \dots, 9\}, p_A = 0.1, N = 1, \gamma = 0.99$
	$z(\cdot 0) = \text{BetaBin}(n = 10, \alpha = 0.7, \beta = 3)$
	$z(\cdot 1) = \text{BetaBin}(n = 10, \alpha = 1, \beta = 0.7)$
Fig. 10	$N = 10, p_A = 0.1, \gamma = 0.99$
	$\pi_{D,1}(S \mathbf{b}_t) = 1 \iff \mathbb{P}[S_t \geq 1 \mathbf{b}_t] \geq 0.75$
	$\pi_{A,1}(S \mathbf{b}_t, s_t) = 0.5$
	Cost function of base strategy estimated using 100 MC samples w. horizon 50
Fig. 14.a-e	$\ell_A = \ell_D = 1, \mathcal{L} = \{1, 2\}, p_A = 1$
	$\pi_{D,1}(S \mathbf{b}_t) = 1 \iff \mathbb{P}[S_t \geq 1 \mathbf{b}_t] \geq 0.75$
	$\pi_{A,1}(S \mathbf{b}_t, s_t) = 0.05$
	$N = 10, \mathcal{O}, z$ (Fig. 13)
	using 100 MC samples w. horizon 50
Fig. 5, Fig. 14.f	\mathcal{O}, z (Fig. 13), $p_A = 0.1, \gamma = 0.99$
	$\mathcal{L} = 0, 1, 2, N = 10$
	$\pi_{D,1}(S \mathbf{b}_t) = 1 \iff \mathbb{P}[S_t \geq 1 \mathbf{b}_t] \geq 0.75$
	$\pi_{A,1}(S \mathbf{b}_t, s_t) = 0.05$
	Best response computation: CEM [50]
	Best responses parameterized following Thm. 1
Fig. 14.g-o, 15	$\ell_A = \ell_D = 1, p_A = 1, \gamma = 0.99$
	$\pi_{D,1}(S \mathbf{b}_t) = 1 \iff \mathbb{P}[S_t \geq 1 \mathbf{b}_t] \geq 0.75$
	$\pi_{A,1}(S \mathbf{b}_t, s_t) = 0.05$
	$N = 10, \mathcal{O}, z$ (Fig. 13)
	using 100 MC samples w. horizon 50
Fig. 14.k	$\Theta_D = \{0, \dots, 200\}$
Table 3	$\ell_A = \ell_D = 1, p_A = 1, \gamma = 0.99$
	$\pi_{D,1}(S \mathbf{b}_t) = 1 \iff \mathbb{P}[S_t \geq 1 \mathbf{b}_t] \geq 0.75$
	$\pi_{A,1}(S \mathbf{b}_t, s_t) = 0.05$
	$N = 10, \mathcal{O}, z$ (Fig. 13, $t = 10$)
	using 100 MC samples w. horizon 50
Fig. 12	$\psi = (\frac{1}{2}, 10^{-2}, -10^5), \chi = (1.0593)$
	$\phi = (-0.5193), \omega = (0.054\pi)$
	time-step: 30s, service time: $\text{Exp}(\mu = 4)t$
Fig. 16	\mathcal{O} (Fig. 13), $\pi_{A,1}(S \cdot) = 1, \ell_D = 1$
Confidence intervals	computed using the Student-t distribution
Base strategies $\pi_{D,1}, \pi_{A,1}$	Approximate threshold best responses against randomized opponents (Fig. 5)
Priors $\mu_1, \rho_1^{(D)}, \rho_1^{(A)}$	uniform
Cost function (7), Fig. 4	$p = 5/4, q = 1, r = 2$
HSVI Parameter	
ϵ	0.1
Cross-entropy method [50]	
λ (fraction of samples to keep)	0.15, 100
K population size	100
M number of samples for each evaluation	50
PPO [75, Alg. 1] parameters	
lr α , batch, # layers, # neurons, clip ϵ	$10^{-5}, 4 \cdot 10^3 t, 4, 64, 0.2,$
GAE λ , ent-coef, activation	$0.95, 10^{-4}, \text{ReLU}$
NFSP [76, Alg. 9] parameters	
lr RL, lr SL, batch, # layers, # neurons, \mathcal{M}_{RL}	$10^{-2}, 5 \cdot 10^{-3}, 64, 2, 128, 2 \times 10^5$
$\mathcal{M}_{SL}, \epsilon, \epsilon$ -decay, η	$2 \times 10^6, 0.06, 0.001, 0.1$

TABLE 5: Hyperparameters.

REFERENCES

- [1] M. H. Manshaei, Q. Zhu, T. Alpcan, T. Basar, and J.-P. Hubaux, "Game theory meets network security and privacy," *ACM Comput. Surv.*, vol. 45, no. 3, pp. 25:1–25:39, Jul. 2013.
- [2] M. van Dijk, A. Juels, A. Oprea, and R. L. Rivest, "Flipit: The game of "stealthy takeover"," *Journal of Cryptology*, no. 4, Oct 2013.
- [3] L. Huang and Q. Zhu, "A dynamic games approach to proactive defense strategies against advanced persistent threats in cyber-physical systems," *Computers & Security*, vol. 89, p. 101660, 11 2019.
- [4] T. Li, Y. Zhao, and Q. Zhu, "The role of information structures in game-theoretic multi-agent learning," *Annual Reviews in Control*, vol. 53, pp. 296–314, 2022.
- [5] C. Kamhoua, C. Kiekintveld, F. Fang, and Q. Zhu, *Game Theory and Machine Learning for Cyber Security*. Wiley, 2021.

ID(s)	Type	Operating system	Zone	Services	Vulnerabilities
1	Gateway	UBUNTU 20	-	SNORT (ruleset v2.9.17.1), SSH, OPENFLOW v1.3, RYU SDN controller	-
2	Gateway	UBUNTU 20	DMZ	SNORT (ruleset v2.9.17.1), SSH, OVS v2.16, OPENFLOW v1.3	-
28	Gateway	UBUNTU 20	R&D	SNORT (ruleset v2.9.17.1), SSH, OVS v2.16, OPENFLOW v1.3	-
3,12	Switch	UBUNTU 22	DMZ	SSH, OPENFLOW v1.3, OVS v2.16	-
21,22	Switch	UBUNTU 22	-	SSH, OPENFLOW v1.3, OVS v2.16	-
23	Switch	UBUNTU 22	ADMIN	SSH, OPENFLOW v1.3, OVS v2.16	-
29-48	Switch	UBUNTU 22	R&D	SSH, OPENFLOW v1.3, OVS v2.16	-
13-16	Honeypot	UBUNTU 20	DMZ	SSH, SNMP, POSTGRES, NTP	-
17-20	Honeypot	UBUNTU 20	DMZ	SSH, IRC, SNMP, SSH, POSTGRES	-
4	App node	UBUNTU 20	DMZ	HTTP, DNS, SSH	CWE-1391
5, 6	App node	UBUNTU 20	DMZ	SSH, SNMP, POSTGRES, NTP	-
7	App node	UBUNTU 20	DMZ	HTTP, TELNET, SSH	CWE-1391
8	App node	DEBIAN JESSIE	DMZ	FTP, SSH, APACHE 2,SNMP	CVE-2015-3306
9,10	App node	UBUNTU 20	DMZ	NTP, IRC, SNMP, SSH, POSTGRES	-
11	App node	DEBIAN JESSIE	DMZ	APACHE 2, SMTP, SSH	CVE-2016-10033
24	Admin system	UBUNTU 20	ADMIN	HTTP, DNS, SSH	CWE-1391
25	Admin system	UBUNTU 20	ADMIN	FTP, MONGODB, SMTP, TOMCAT, TS 3, SSH	-
26	Admin system	UBUNTU 20	ADMIN	SSH, SNMP, POSTGRES, NTP	-
27	Admin system	UBUNTU 20	ADMIN	FTP, MONGODB, SMTP, TOMCAT, TS 3, SSH	CWE-1391
49-59	Compute node	UBUNTU 20	R&D	SPARK, HDFS	-
60	Compute node	DEBIAN WHEEZY	R&D	SPARK, HDFS, APACHE 2,SNMP, SSH	CVE-2014-6271
61	Compute node	DEBIAN 9.2	R&D	IRC, APACHE 2, SSH	CWE-89
62	Compute node	DEBIAN JESSIE	R&D	SPARK, HDFS, TS 3, TOMCAT, SSH	CVE-2010-0426
63	Compute node	DEBIAN JESSIE	R&D	SSH, SPARK, HDFS	CVE-2015-5602
64	Compute node	DEBIAN JESSIE	R&D	SAMBA, NTP, SSH, SPARK, HDFS	CVE-2017-7494

TABLE 6: Configuration of the target infrastructure shown in Fig. 1; vulnerabilities in specific software products are identified by the vulnerability identifiers in the Common Vulnerabilities and Exposures (CVE) database [66]; vulnerabilities that are not described in the CVE database are categorized according to the types of the vulnerabilities they exploit based on the Common Weakness Enumeration (CWE) list [67].

- [6] K. Durkota, V. Lisy, B. Bořanský, and C. Kiekintveld, "Optimal network security hardening using attack graph games," in *Proceedings of the 24th International Conference on Artificial Intelligence*, 2015.
- [7] K. Horák, B. Bosanský, P. Tomásek, C. Kiekintveld, and C. A. Kamhoua, "Optimizing honeypot strategies against dynamic lateral movement using partially observable stochastic games," *Comput. Secur.*, vol. 87, 2019.
- [8] K. Hammar and R. Stadler, "Learning near-optimal intrusion responses against dynamic attackers," *IEEE Transactions on Network and Service Management*, vol. 21, no. 1, pp. 1158–1177, 2024.
- [9] —, "Scalable learning of intrusion response through recursive decomposition," in *Decision and Game Theory for Security*, J. Fu, T. Kroupa, and Y. Hayel, Eds. Cham: Springer Nature Switzerland, 2023, pp. 172–192.
- [10] Y. Zhao, L. Huang, C. Smidts, and Q. Zhu, "Finite-horizon semi-markov game for time-sensitive attack response and probabilistic risk assessment in nuclear power plants," *Reliability Engineering & System Safety*, vol. 201, p. 106878, 2020.
- [11] J. Chen and Q. Zhu, "Interdependent strategic security risk management with bounded rationality in the internet of things," *IEEE Transactions on Information Forensics and Security*, vol. 14, no. 11, pp. 2958–2971, 2019.
- [12] U. D. of Justice, "Six russian gru officers charged in connection with worldwide deployment of destructive malware and other disruptive actions in cyberspace," 2020, <https://www.justice.gov/opa/pr/six-russian-gru-officers-charged-connection-worldwide-deployment-destructive-malware-and>.
- [13] T. M. Corporation, "Notpetya," 2024, <https://attack.mitre.org/software/S0368/>.
- [14] D. Bertsekas, *Rollout, Policy Iteration, and Distributed Reinforcement Learning*, ser. Athena scientific optimization and computation series. Athena Scientific, 2021.
- [15] I. Esponda and D. Pouzo, "Berk-nash equilibrium: A framework for modeling agents with misspecified models," *Econometrica*, vol. 84, no. 3, pp. 1093–1130, 2023/10/13/ 2016.
- [16] J. H. Kagel and D. Levin, "The winner's curse and public information in common value auctions," *The American Economic Review*, vol. 76, no. 5, pp. 894–920, 1986.
- [17] M. Rabin, "Inference by believers in the law of small numbers," *The Quarterly Journal of Economics*, vol. 117, no. 3, pp. 775–816, 2002.
- [18] H. A. Simon, "Theories of bounded rationality," *Decision and Organization*, pp. 161–176, 1972.
- [19] L. Samuelson, "Bounded rationality and game theory," *The Quarterly Review of Economics and Finance*, vol. 36, no. Supplemen, pp. 17–35, 1996.
- [20] R. W. Rosenthal, "A bounded-rationality approach to the study of noncooperative games," *International Journal of Game Theory*, vol. 18, no. 3, pp. 273–292, Sep 1989.
- [21] A. Sanjab, W. Saad, and T. Başar, "A game of drones: Cyber-physical security of time-critical uav applications with cumulative prospect theory perceptions and valuations," *IEEE Transactions on Communications*, vol. 68, no. 11, pp. 6990–7006, 2020.
- [22] R. Gabrys, M. Bilinski, J. Mauger, D. Silva, and S. Fugate, "Casino rationale: Countering attacker deception in zero-sum stackelberg security games of bounded rationality," in *Decision and Game Theory for Security*, F. Fang, H. Xu, and Y. Hayel, Eds. Cham: Springer International Publishing, 2023, pp. 23–43.
- [23] J. Chen and Q. Zhu, "Security investment under cognitive constraints: A gestalt nash equilibrium approach," in *2018 52nd Annual Conference on Information Sciences and Systems (CISS)*, 2018, pp. 1–6.
- [24] A. Sinha, F. Fang, B. An, C. Kiekintveld, and M. Tambe, "Stackelberg security games: Looking beyond a decade of success," in *Proceedings of the Twenty-Seventh International Joint Conference on Artificial Intelligence, IJCAI-18*. International Joint Conferences on Artificial Intelligence Organization, 7 2018, pp. 5494–5501.
- [25] Z. Wan, J.-H. Cho, M. Zhu, A. H. Anwar, C. A. Kamhoua, and M. P. Singh, "Foureye: Defensive deception against advanced persistent threats via hypergame theory," *IEEE Transactions on Network and Service Management*, vol. 19, no. 1, pp. 112–129, 2022.
- [26] C. Bakker, A. Bhattacharya, S. Chatterjee, and D. L. Vrable, "Learning and information manipulation: Repeated hypergames for cyber-physical security," *IEEE Control Systems Letters*, vol. 4, no. 2, pp. 295–300, 2020.
- [27] M. Abdallah, P. Naghizadeh, A. R. Hota, T. Cason, S. Bagchi, and S. Sundaram, "Behavioral and game-theoretic security investments in interdependent systems modeled by attack graphs," *IEEE Transactions on Control of Network Systems*, vol. 7, no. 4, pp. 1585–1596, 2020.
- [28] C. N. Mavridis, A. Kanellopoulos, K. G. Vamvoudakis, J. S. Baras, and K. H. Johansson, "Attack identification for cyber-physical security in dynamic games under cognitive hierarchy," *IFAC-PapersOnLine*, vol. 56, no. 2, pp. 11 223–11 228, 2023, 22nd IFAC World Congress.
- [29] O. Tsemogne, Y. Hayel, C. Kamhoua, and G. Deugoue, "Partially observable stochastic games for cyber deception against network epidemic," in *Decision and Game Theory for Security*, Q. Zhu, J. S.

- Baras, R. Poovendran, and J. Chen, Eds. Cham: Springer International Publishing, 2020, pp. 312–325.
- [30] K. Hammar and R. Stadler, “Finding effective security strategies through reinforcement learning and Self-Play,” in *International Conference on Network and Service Management (CNSM 2020)*, Izmir, Turkey, 2020.
- [31] A. Aydeger, M. H. Manshaei, M. A. Rahman, and K. Akkaya, “Strategic defense against stealthy link flooding attacks: A signaling game approach,” *IEEE Transactions on Network Science and Engineering*, vol. 8, no. 1, pp. 751–764, 2021.
- [32] T. Alpcan and T. Basar, *Network Security: A Decision and Game-Theoretic Approach*, 1st ed. USA: Cambridge University Press, 2010.
- [33] D. Fudenberg and D. K. Levine, *The theory of learning in games*. MIT Press, Cambridge, MA., 1998.
- [34] H. P. Young, *Strategic learning and its limits*. Oxford University Press, 2004, cited by 0313.
- [35] J. Hu and M. P. Wellman, “Nash q-learning for general-sum stochastic games,” *J. Mach. Learn. Res.*, vol. 4, no. null, p. 1039–1069, dec 2003.
- [36] M. L. Littman, “Markov games as a framework for multi-agent reinforcement learning,” in *Proceedings of the Eleventh International Conference on International Conference on Machine Learning*, ser. ICML’94. San Francisco, CA, USA: Morgan Kaufmann Publishers Inc., 1994, p. 157–163.
- [37] Y. Ge, T. Li, and Q. Zhu, “Scenario-agnostic zero-trust defense with explainable threshold policy: A meta-learning approach,” *IEEE INFOCOM 2023 - IEEE Conference on Computer Communications Workshops (INFOCOM WKSHPS)*, pp. 1–6, 2023.
- [38] K. Hammar and R. Stadler, “Intrusion prevention through optimal stopping,” *IEEE Transactions on Network and Service Management*, vol. 19, no. 3, pp. 2333–2348, 2022.
- [39] S. Acharya, Y. Dvorkin, and R. Karri, “Causative cyberattacks on online learning-based automated demand response systems,” *IEEE Transactions on Smart Grid*, vol. 12, no. 4, pp. 3548–3559, 2021.
- [40] CSLE, “Cyber security learning environment,” 2023, documentation: <https://limmen.dev/csle/>, traces: <https://github.com/Limmen/csle/releases/tag/v0.4.0>, source code: <https://github.com/Limmen/csle>, video demonstration: <https://www.youtube.com/watch?v=iE2KPmtIs2A&>.
- [41] M. Roesch, “Snort - lightweight intrusion detection for networks,” in *Proceedings of the 13th USENIX Conference on System Administration*, ser. LISA ’99. USA: USENIX Association, 1999, p. 229–238.
- [42] S. Moothedath, D. Sahabandu, J. Allen, A. Clark, L. Bushnell, W. Lee, and R. Poovendran, “A game-theoretic approach for dynamic information flow tracking to detect multistage advanced persistent threats,” *IEEE Transactions on Automatic Control*, vol. 65, no. 12, pp. 5248–5263, 2020.
- [43] K. Horák, B. Bošanský, V. Kovařík, and C. Kiekintveld, “Solving zero-sum one-sided partially observable stochastic games,” *Artificial Intelligence*, vol. 316, p. 103838, 2023.
- [44] Y. Ji, S. Lee, M. Fazzini, J. Allen, E. Downing, T. Kim, A. Orso, and W. Lee, “Enabling refinable Cross-Host attack investigation with efficient data flow tagging and tracking,” in *27th USENIX Security Symposium (USENIX Security 18)*. Baltimore, MD: USENIX Association, Aug. 2018, pp. 1705–1722.
- [45] J. Goldsmith and M. Mundhenk, “Competition adds complexity,” in *Advances in Neural Information Processing Systems*, J. Platt, D. Koller, Y. Singer, and S. Roweis, Eds., vol. 20. Curran Associates, Inc., 2007.
- [46] K. Horák, “Scalable algorithms for solving stochastic games with limited partial observability,” Ph.D. dissertation, Czech Technical University in Prague, 2019.
- [47] H. W. Kuhn, *Extensive games and the problem of information*, H. W. Kuhn and A. W. Tucker, Eds. Princeton, NJ: Princeton University Press, 1953.
- [48] P. R. Kumar and P. Varaiya, *Stochastic systems: estimation, identification and adaptive control*. USA: Prentice-Hall, Inc., 1986.
- [49] V. Krishnamurthy, *Partially Observed Markov Decision Processes: From Filtering to Controlled Sensing*. Cambridge University Press, 2016.
- [50] R. Rubinstein, “The cross-entropy method for combinatorial and continuous optimization,” *Methodology And Computing In Applied Probability*, vol. 1, no. 2, pp. 127–190, Sep 1999.
- [51] J. F. Nash, “Non-cooperative games,” *Annals of Mathematics*, vol. 54, pp. 286–295, 1951.
- [52] J. von Neumann, “Zur Theorie der Gesellschaftsspiele. (German) [On the theory of games of strategy],” *j-MATH-ANN*, vol. 100, pp. 295–320, 1928.
- [53] D. Fudenberg and J. Tirole, *Game Theory*. MIT Press, 1991.
- [54] I.-K. Cho and D. M. Kreps, “Signaling games and stable equilibria,” *The Quarterly Journal of Economics*, vol. 102, no. 2, pp. 179–221, 1987.
- [55] S. Banach, “Sur les opérations dans les ensembles abstraits et leur application aux équations intégrales,” *Fundamenta Mathematicae*, 1922.
- [56] J. Hespanha and M. Prandini, “Nash equilibria in partial-information games on markov chains,” in *Proceedings of the 40th IEEE Conference on Decision and Control (Cat. No.01CH37228)*, vol. 3, 2001.
- [57] K. Horák, B. Bošanský, and M. Pěchouček, “Heuristic search value iteration for one-sided partially observable stochastic games,” *Proceedings of the AAAI Conference on Artificial Intelligence*, Feb. 2017.
- [58] E. J. Sondik, “The optimal control of partially observable markov processes over the infinite horizon: Discounted costs,” *Operations Research*, vol. 26, no. 2, pp. 282–304, 1978.
- [59] M. L. Puterman, *Markov Decision Processes: Discrete Stochastic Dynamic Programming*, 1st ed. USA: Wiley, 1994.
- [60] S. Bhattacharya, S. Badyal, T. Wheeler, S. Gil, and D. Bertsekas, “Reinforcement learning for pomdp: Partitioned rollout and policy iteration with application to autonomous sequential repair problems,” *IEEE Robotics and Automation Letters*, vol. 5, no. 3, pp. 3967–3974, 2020.
- [61] S. Kullback and R. A. Leibler, “On information and sufficiency,” *The Annals of Mathematical Statistics*, vol. 22, no. 1, pp. 79–86, 1951.
- [62] R. H. Berk, “Limiting Behavior of Posterior Distributions when the Model is Incorrect,” *The Annals of Mathematical Statistics*, vol. 37, no. 1, pp. 51 – 58, 1966.
- [63] I. Esponda and D. Pouzo, “Equilibrium in misspecified Markov decision processes,” *Theoretical Economics*, vol. 16, no. 2, pp. 717–757, 2021.
- [64] S. Hemminger, “Network emulation with netem,” *Linux Conf*, 2005.
- [65] H. P. Reiser and R. Kapitzka, “Hypervisor-based efficient proactive recovery,” in *2007 26th IEEE International Symposium on Reliable Distributed Systems (SRDS 2007)*, 2007, pp. 83–92.
- [66] T. M. Corporation, “Cve database,” 2022, <https://cve.mitre.org/>.
- [67] —, “Cwe list,” 2023, <https://cwe.mitre.org/index.html>.
- [68] B. E. Strom, A. Applebaum, D. P. Miller, K. C. Nickels, A. G. Pennington, and C. B. Thomas, “Mitre att&ck: Design and philosophy,” in *Technical report*. The MITRE Corporation, 2018.
- [69] M. Kuhl, J. Wilson, and M. Johnson, “Estimation and simulation of nonhomogeneous poisson processes having multiple periodicities,” in *Winter Simulation Conference Proceedings, 1995.*, 1995, pp. 374–383.
- [70] D. Ford, F. Labelle, F. Popovici, M. Stokely, V.-A. Truong, L. Barroso, C. Grimes, and S. Quinlan, “Availability in globally distributed storage systems,” in *Proceedings of the 9th USENIX Symposium on Operating Systems Design and Implementation*, 2010.
- [71] M. Shen and J. P. How, “Robust opponent modeling via adversarial ensemble reinforcement learning,” *Proceedings of the International Conference on Automated Planning and Scheduling*, vol. 31, no. 1, pp. 578–587, May 2021.
- [72] N. Nisan, T. Roughgarden, E. Tardos, and V. V. Vazirani, *Algorithmic Game Theory*. New York, NY, USA: Cambridge University Press, 2007.
- [73] D. Hernandez, K. Denamganai, Y. Gao, P. York, S. Devlin, S. Samothrakakis, and J. A. Walker, “A generalized framework for self-play training,” in *2019 IEEE Conference on Games (CoG)*, 2019, pp. 1–8.
- [74] G. W. Brown, “Iterative solution of games by fictitious play,” 1951, activity analysis of production and allocation.
- [75] J. Schulman, F. Wolski, P. Dhariwal, A. Radford, and O. Klimov, “Proximal policy optimization algorithms,” *CoRR*, 2017, <http://arxiv.org/abs/1707.06347>.
- [76] J. Heinrich, “Reinforcement learning from self-play in imperfect-information games,” Ph.D. dissertation, University College London, 2017.
- [77] M. Tambe, *Security and Game Theory: Algorithms, Deployed Systems, Lessons Learned*, 1st ed. USA: Cambridge University Press, 2011.
- [78] J. Tan, H. Jin, H. Zhang, Y. Zhang, D. Chang, X. Liu, and H. Zhang, “A survey: When moving target defense meets game theory,” *Computer Science Review*, vol. 48, p. 100544, 2023.
- [79] T. T. Nguyen and V. J. Reddi, “Deep reinforcement learning for cyber security,” *IEEE Transactions on Neural Networks and Learning Systems*, vol. 34, no. 8, pp. 3779–3795, 2023.
- [80] L.-X. Yang, P. Li, Y. Zhang, X. Yang, Y. Xiang, and W. Zhou, “Effective repair strategy against advanced persistent threat: A differential game approach,” *IEEE Transactions on Information Forensics and Security*, vol. 14, no. 7, pp. 1713–1728, 2019.

- [81] H. Sun, X. Yang, L.-X. Yang, K. Huang, and G. Li, "Impulsive artificial defense against advanced persistent threat," *IEEE Transactions on Information Forensics and Security*, vol. 18, pp. 3506–3516, 2023.
- [82] T. Zhu, D. Ye, Z. Cheng, W. Zhou, and P. S. Yu, "Learning games for defending advanced persistent threats in cyber systems," *IEEE Transactions on Systems, Man, and Cybernetics: Systems*, 2022.
- [83] E. Altman, K. Avrachenkov, and A. Garnaev, "A jamming game in wireless networks with transmission cost," in *NET-COOP*, 2007.
- [84] T. Halabi, O. A. Wahab, R. Al Mallah, and M. Zulkermine, "Protecting the internet of vehicles against advanced persistent threats: A bayesian stackelberg game," *IEEE Transactions on Reliability*, vol. 70, no. 3, pp. 970–985, 2021.
- [85] J. Tan, H. Jin, H. Hu, R. Hu, H. Zhang, and H. Zhang, "Wf-mtd: Evolutionary decision method for moving target defense based on wright-fisher process," *IEEE Transactions on Dependable and Secure Computing*, vol. 20, no. 6, pp. 4719–4732, 2023.
- [86] K. C. Nguyen, T. Alpcan, and T. Basar, "Stochastic games for security in networks with interdependent nodes," in *2009 International Conference on Game Theory for Networks*, 2009, pp. 697–703.
- [87] Q. Zhu and T. Başar, "Dynamic policy-based ids configuration," in *Proceedings of the 48th IEEE Conference on Decision and Control (CDC) held jointly with 2009 28th Chinese Control Conference*, 2009.
- [88] H. Hu, Y. Liu, C. Chen, H. Zhang, and Y. Liu, "Optimal decision making approach for cyber security defense using evolutionary game," *IEEE Transactions on Network and Service Management*, vol. 17, no. 3, pp. 1683–1700, 2020.
- [89] S. A. Zonouz, H. Khurana, W. H. Sanders, and T. M. Yardley, "Rre: A game-theoretic intrusion response and recovery engine," in *2009 IEEE/IFIP International Conference on Dependable Systems & Networks*, 2009, pp. 439–448.
- [90] Y. Zhang, J. Liu, and A. S. Namin, "Optimal decision-making approach for cyber security defense using game theory and intelligent learning," *Sec. and Commun. Netw.*, vol. 2019, jan 2019.
- [91] H. Zhang, Y. Mi, X. Liu, Y. Zhang, J. Wang, and J. Tan, "A differential game approach for real-time security defense decision in scale-free networks," *Computer Networks*, vol. 224, p. 109635, 2023.
- [92] X. Liu, H. Zhang, Y. Zhang, L. Shao, and J. Han, "Active defense strategy selection method based on two-way signaling game," *Security and Communication Networks*, vol. 2019, pp. 1–14, 11 2019.
- [93] M.-F. Balcan, A. Blum, N. Haghtalab, and A. D. Procaccia, "Commitment without regrets: Online learning in stackelberg security games," in *Proceedings of the Sixteenth ACM Conference on Economics and Computation*, ser. EC '15. New York, NY, USA: Association for Computing Machinery, 2015, p. 61–78.
- [94] V. Lisy, T. Davis, and M. Bowling, "Counterfactual regret minimization in sequential security games," *Proceedings of the AAI Conference on Artificial Intelligence*, vol. 30, no. 1, Feb. 2016.
- [95] L. Huang and Q. Zhu, "A dynamic games approach to proactive defense strategies against advanced persistent threats in cyber-physical systems," *Computers & Security*, vol. 89, p. 101660, 2020.
- [96] J. Harsanyi, "Games with incomplete information played by "bayesian" players, i-iii part i. the basic model," *Management Science*, vol. 14, no. 3, pp. 159–182, 1967.
- [97] H. A. Simon, "A behavioral model of rational choice," *The Quarterly Journal of Economics*, vol. 69, no. 1, pp. 99–118, 1955.
- [98] Z. Ni and S. Paul, "A multistage game in smart grid security: A reinforcement learning solution," *IEEE Transactions on Neural Networks and Learning Systems*, vol. 30, no. 9, pp. 2684–2695, 2019.
- [99] M. Yin, T. Li, H. Lei, Y. Hu, S. Rangan, and Q. Zhu, "Zero-shot wireless indoor navigation through physics-informed reinforcement learning," 2023, <https://arxiv.org/abs/2306.06766>.
- [100] G. Farina and T. Sandholm, "Model-free online learning in unknown sequential decision making problems and games," *Proceedings of the AAI Conference on Artificial Intelligence*, vol. 35, no. 6, pp. 5381–5390, May 2021.
- [101] R. Bellman, "A markovian decision process," *Journal of Mathematics and Mechanics*, vol. 6, no. 5, pp. 679–684, 1957.
- [102] D. Bertsekas, *Reinforcement learning and optimal control*. Athena Scientific, 2019.
- [103] R. B. Ash and C. Doléans-Dade, *Probability and Measure Theory*, ser. Academic Press. Academic Press, 2000.
- [104] C. T. Ionescu Tulcea, "Mesures dans les espaces produits," *Lincei-Rend. Sc. fis. mat. e nat.*, vol. 7, pp. 208–211, 1949.
- [105] D. Pollard, *A User's Guide to Measure Theoretic Probability*, ser. Cambridge Series in Statistical and Probabilistic Mathematics. Cambridge University Press, 2001.
- [106] P. Billingsley, *Convergence of probability measures*, 2nd ed., ser. Wiley Series in Probability and Statistics: Probability and Statistics. New York: John Wiley & Sons Inc., 1999, a Wiley-Interscience Publication.
- [107] C. D. Aliprantis and K. C. Border, *Infinite Dimensional Analysis: a Hitchhiker's Guide*. Berlin; London: Springer, 2006.